

8-2010

AN IMPLANTABLE MOSFET DOSIMETER MODIFIED TO ACT AS A FIDUCIAL MARKER

Joseph S. Dick

Follow this and additional works at: https://digitalcommons.library.tmc.edu/utgsbs_dissertations



Part of the [Other Medical Sciences Commons](#), [Other Physics Commons](#), and the [Radiology Commons](#)

Recommended Citation

Dick, Joseph S., "AN IMPLANTABLE MOSFET DOSIMETER MODIFIED TO ACT AS A FIDUCIAL MARKER" (2010). *The University of Texas MD Anderson Cancer Center UTHealth Graduate School of Biomedical Sciences Dissertations and Theses (Open Access)*. 65.

https://digitalcommons.library.tmc.edu/utgsbs_dissertations/65

This Thesis (MS) is brought to you for free and open access by the The University of Texas MD Anderson Cancer Center UTHealth Graduate School of Biomedical Sciences at DigitalCommons@TMC. It has been accepted for inclusion in The University of Texas MD Anderson Cancer Center UTHealth Graduate School of Biomedical Sciences Dissertations and Theses (Open Access) by an authorized administrator of DigitalCommons@TMC. For more information, please contact digitalcommons@library.tmc.edu.

AN IMPLANTABLE MOSFET DOSIMETER MODIFIED TO ACT AS A FIDUCIAL
MARKER

by

Joseph Stevenson Dick, B.S., B.S.B.A.

APPROVED:

Mohammad Salehpour, Supervisory Professor

Sean Zhang

Firas Mourtada

R. Allen White

Gloria Beyer

APPROVED:

Dean, The University of Texas

Graduate School of Biomedical Sciences at Houston

AN IMPLANTABLE MOSFET DOSIMETER MODIFIED TO ACT AS A FIDUCIAL
MARKER

A

THESIS

Presented to the Faculty of

The University of Texas

Health Science Center at Houston

and

The University of Texas

M. D. Anderson Cancer Center

Graduate School of Biomedical Sciences

in Partial Fulfillment

of the Requirements

for the Degree of

MASTER OF SCIENCE

by

Joseph Stevenson Dick, B.S., B.S.B.A.

Houston, Texas

August 2010

ABSTRACT

In external beam radiation therapy, it is imperative that the prescribed dose is administered to the correct location and in the correct amount. Though several *ex vivo* methods of quality assurance are currently employed to achieve this goal, verifying that the correct dose is received within the patient *in situ* is impossible without the capability of measuring dose inside the patient. Recently, a method of measuring dose delivered within the patient has been developed, an implantable MOSFET dosimeter. This dosimeter is implanted within the patient and records the dose received. Since the dosimeter is implanted in the patient, it could serve a dual function as a fiducial marker for image guided radiation therapy (IGRT) treatment if it could be modified to be visible on x-rays. In this study, modifications to the MOSFET dosimeter were made to increase its visibility for IGRT treatment. To test whether the modifications hindered the dosimeter's ability to accurately measure and transmit dose information, the energy dependence, angular dependence and wireless read range of the modified dosimeter were measured and compared to unmodified dosimeters. It was found that the modified dosimeter performed as well as the unmodified dosimeter while also being suitable for use as a fiducial marker for IGRT treatment.

TABLE OF CONTENTS

INTRODUCTION	1
BACKGROUND	3
Dose Verification System	3
MOSFET Dosimetry	4
MOSFET Fading Effect	6
Previous Work with the DVS Dosimeter (original 25mm dosimeter).....	6
Previous Work with the DVS Dosimeter (new 20mm dosimeter).....	10
DVS Dosimeter (new 20mm dosimeter) in other radiotherapy treatment modalities .	12
Using the DVS dosimeter as a fiducial marker	14
METHODS AND MATERIALS	15
Prototype Dosimeters	15
Imaging – Prototype Visualization Study	16
Modified Dosimeter	17
Imaging – Controlled Study	18
Wireless Reader	19
Data Acquisition – Compensating for the Calibration Curve	20
Read Range Study	22
Energy Dependence Study	23
Angular Dependence Temperature Control Apparatus.....	25

Angle Definition	26
Angular Dependence Study	27
RESULTS AND DISCUSSION.....	29
Imaging – Prototype Visualization Study	29
Imaging – Controlled Study	35
Read Range Study	47
Energy Dependence Study	47
Rotational Angular Dependence Study.....	49
Longitudinal Angular Dependence Study.....	52
Azimuthal Angular Dependence.....	53
CONCLUSIONS	55
Suitability of Modified Dosimeter as a Fiducial Marker	55
Effect of Modification on Dosimeter Properties.....	55
Future Work	56
Recommendations.....	56
BIBLIOGRAPHY.....	57
VITA.....	60

LIST OF ILLUSTRATIONS

Figure 1 - The DVS dosimeter is 20mm in length and 2.1mm in diameter. It contains two MOSFETs 1.3mm from the end of the dosimeter that measure dose. Source: Sicel Technologies Product Info Sheet. Used with permission.....	3
Figure 2 – The wireless dosimeter reader produces a wave that induces a current in the dosimeter and receives the dosimeter’s measurements.	3
Figure 3 - Ionizing Radiation increases positive charge in the gate-oxide layer changing the threshold voltage of the MOSFET.....	4
Figure 4 – Threshold Voltage shift versus Accumulated Dose as measured by Scarantino (2004). Used with Permission.....	6
Figure 5 - Briere <i>et al.</i> 's measurement of rotational angular dependence (Briere 2007). Used with Permission.	10
Figure 6 - Beyer <i>et al.</i> 's measurement of rotational (a) and longitudinal (b) angular dependence. Used with permission (Beyer 2008). Copyright 2008 IEEE.	11
Figure 7 - Fagerstrom <i>et al.</i> 's rotational angular dependence results (Fagerstrom 2008)	13
Figure 8 - Fagerstrom <i>et al.</i> 's longitudinal angular dependence (Fagerstrom 2008). Used with Permission.	13
Figure 9 - Prototype Dosimeters Standard (A) Gold Sleeve (B) and Wire Wrapped (C)	15
Figure 10 - Pelvic section of Rando phantom used for preliminary imaging study	16
Figure 11 - Modified dosimeter (far left) in comparison with the current commercially available dosimeter. U.S. dime included for size comparison.....	17
Figure 12 - Pelvic section of Rando phantom used for controlled imaging study	18
Figure 13 - Bar Code Reader (top) and sample bar code (bottom)	19

Figure 14 - Sample data analysis. Fractions 1,3,5 represent reference value of 0°.	
Fractions 2,4 represent test values in the rotational angular study of 40°, 80°, respectively.	21
Figure 15 - Dosimeter holder with three DVS dosimeters.	22
Figure 16 - Dosimeter holder in water tank. The tube end of the dosimeter holder is the same size as the ionization chamber used in the tank allowing the MOSFET readings to be compared with absolute dose measurements.	23
Figure 17 – The water tank is shown with heater apparatus and circulating pump.....	23
Figure 18 – Temperature controlled water supply flowed through all phantoms used in this study to keep the MOSFETs at 37° C.	25
Figure 19 - Angle Definition	26
Figure 20 - Spherical Phantom (top) close-up of insert (middle; dosimeter identified with dashed circle) and close-up of side of phantom showing how insert can be rotated (bottom)	27
Figure 21 - kV AP View of Prototype Visualization Study. From top left to bottom right: E (1.2mm Gold Marker), D (25mm Dosimeter with Marker), F (0.8mm Gold Marker), B (Gold Sleeve Modified Dosimeter), A (Standard Dosimeter), C (Wire Wrapped Modified Dosimeter).....	30
Figure 22 - MV AP View of Prototype Visualization Study. From top left to bottom right: E (1.2mm Gold Marker), D (25mm Dosimeter with Marker), F (0.8mm Gold Marker), B (Gold Sleeve Modified Dosimeter), A (Standard Dosimeter),C (Wire Wrapped Modified Dosimeter).....	31

Figure 23 - kV Lateral View of Prototype Visualization Study. From top left to bottom right: D (25mm Dosimeter with Marker), E (1.2mm Gold Marker), F (0.8mm Gold Marker), A (Standard Dosimeter), B (Gold Sleeve Modified Dosimeter), C (Wire Wrapped Modified Dosimeter).....	32
Figure 24 - MV Lateral View of Prototype Visualization Study. From left to right: F (0.8mm Gold Marker), E (1.2mm Gold Marker), D (25mm Dosimeter with Marker). Markers A – C unviewable due to streak.....	33
Figure 25 - CBCT Slice of Prototype Visualization Study. Top Image left to right: E (1.2mm Gold Marker), D (25mm Dosimeter with Marker), F (0.8mm Gold Marker). Bottom Image left to right: B (Gold Sleeve Modified Dosimeter), A (Standard Dosimeter), C (Wire Wrapped Modified Dosimeter).....	34
Figure 26 - kV AP images. From top left to bottom right: Commercially Available Dosimeter, Modified Dosimeter, Gold Marker, Carbon Marker.....	37
Figure 27 - MV AP images. From top left to bottom right: Commercially Available Dosimeter, Modified Dosimeter, Gold Marker, Carbon Marker.....	38
Figure 28 - MV AP images Magnified. From top to bottom: Commercially Available Dosimeter, Modified Dosimeter, Gold Marker, Carbon Marker.....	39
Figure 29 - kV Lateral images. From top to bottom: Commercially Available Dosimeter, Modified Dosimeter, Gold Marker, Carbon Marker	40
Figure 30 - MV Lateral images. From top left to bottom right: Commercially Available Dosimeter, Modified Dosimeter, Gold Marker, Carbon Marker.....	41
Figure 31 - CBCT Slice of Commercial Dosimeter (top), Modified Dosimeter (bottom)	42

Figure 32 - CBCT Slice of Gold Marker (top), Carbon Marker (bottom).....	43
Figure 33 - Line profiles of the AP images. The gold marker and modified dosimeter show comparable results.....	44
Figure 34 - Line profiles of the lateral images. The gold marker and modified dosimeter show comparable results.....	45
Figure 35 - Rotational Angular Dependence	50

LIST OF TABLES

Table 1 - Legend for Prototype Visualization Images and Average Pixel Difference from Background on MV AP image	29
Table 2 - Results of the Energy Dependence Study for both the commercial and modified dosimeter	48
Table 3 - Rotational Angular Dependence of both the Commercial and Modified Dosimeters	49
Table 4 - Longitudinal Angular Dependence of both the Commercial and Modified Dosimeter.....	52
Table 5 - Azimuthal Angular Dependence of both the Commercial and Modified Dosimeters. The data is reported relative to a 0° rotation, 0° longitudinal angle	53
Table 6 - Azimuthal Angular Dependence for both the Commercial and Modified Dosimeter. Data presented is the difference between the angular readings and the Azimuthal 0° angular reading.	54

ABBREVIATIONS

AP = anteroposterior

CBCT = cone beam computed tomography

CT = computed tomography

DVS = Dose Verification System (the brand name of the MOSFET based dosimeters used in this research)

IGRT = image guided radiation therapy

kV = kilovoltage

linac = linear accelerator

MOSFET = Metal Oxide Semiconductor Field Effect Transistor

MV = megavoltage

OBI = On Board Imager® (the imaging system on a linac which is used for patient alignment in image guided radiation therapy)

ROI = Region of Interest

TG51 = Task Group #51

INTRODUCTION

For patients receiving radiation therapy, accurate and consistent delivery of dose is of the utmost importance. Several publications have directly linked the accuracy and consistency of daily dose delivery with tumor control probabilities (for example, Brahme 1984, Bortfeld 2006). Several methods are utilized in the practice of radiation therapy to ensure accurate and consistent daily dose delivery. These methods include utilizing patient immobilization devices, creating reproducible setups and performing quality assurance measurements of the radiation treatment machines. For disease sites where internal anatomy is expected to shift relative to external markers, image guided radiation therapy (IGRT) can be used in addition to the above techniques to further ensure a consistent setup. In IGRT, an image of the area to be treated (in the case of this thesis, an x-ray) is acquired while the patient is on the treatment table in the proper setup position before beginning each treatment session. One such image, a megavoltage (MV) portal image can be acquired by adding a detector to the gantry of the linear accelerator (linac) and using the linac itself as the x-ray source. Since MV level x-rays are limited in their contrast, some choose to add a kilovoltage (kV) source and detector to the linac, which can be used to generate a kV image or a cone-beam computed tomography image (CBCT). Whatever types of images are acquired, they are compared to digitally reconstructed radiographs generated from the treatment plan and a shift is made to correct for any discrepancies in patient alignment. However, the quality of the x-rays taken can hinder proper alignment. When aligning to a soft-tissue structure that is difficult or impossible to see on an x-ray, a fiducial marker, typically a small piece of gold or other high-Z material is implanted in the patient to assist the radiation therapy

technician with alignment. The high density of a gold marker makes it visible on even the relatively low-contrast MV images.

Through IGRT and reproducible patient setups, we can verify that the patient is set up consistently, but the dose received cannot be verified without a way to measure radiation within the patient. Recently, a method of measuring dose within a patient has been developed. The Dose Verification System (DVS; Sixel Technologies, Morrisville, NC) is a permanently implantable radiation dosimeter designed to be implanted in a patient near the treatment site and to measure the dose delivered. This measurement is extremely valuable in ensuring that the treatment plan is being delivered as prescribed. Since, like a fiducial marker, the DVS dosimeter has to be implanted within the patient, it would be ideal to have the DVS dosimeter act as the fiducial marker. If possible, this combination would save the patient an additional implantation and would allow the advantages of the Dose Verification System to be combined with the advantages of IGRT treatment.

Unfortunately, the current design of the DVS dosimeter, though visible on kV images cannot be seen on an MV portal image. In order to be visible on an MV image, the existing dosimeter would have to be modified, but the modification would have to be done in such a way as to not hinder the dosimeter's measurement ability. The investigation of how to modify the dosimeter, and the subsequent testing of the new modified dosimeter's measurement characteristics and its suitability for IGRT treatments is the subject of this thesis.

BACKGROUND

Dose Verification System

The Dose Verification System (DVS; Sichel Technologies, Morrisville, NC) consists of a permanently implantable dosimeter (Figure 1) and a wireless reader (Figure 2). The dose is measured using metal oxide semiconductor field effect transistors (MOSFETs) within the dosimeter. The MOSFETs used in the DVS dosimeter have a sensitive volume of 0.3mm x 0.05mm and comprise only a small portion of the dosimeter. The remainder of the dosimeter is composed of electronic circuitry and an antenna. When a dosimeter is to be read, the wand portion of the reader generates an electromagnetic field. This field powers the dosimeter via its antenna. The electronic

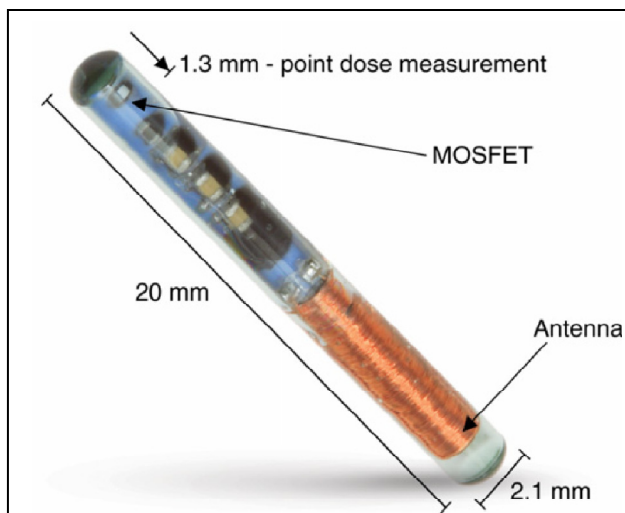


Figure 1 - The DVS dosimeter is 20mm in length and 2.1mm in diameter. It contains two MOSFETs 1.3mm from the end of the dosimeter that measure dose. Source: Sichel Technologies Product Info Sheet. Used with permission.



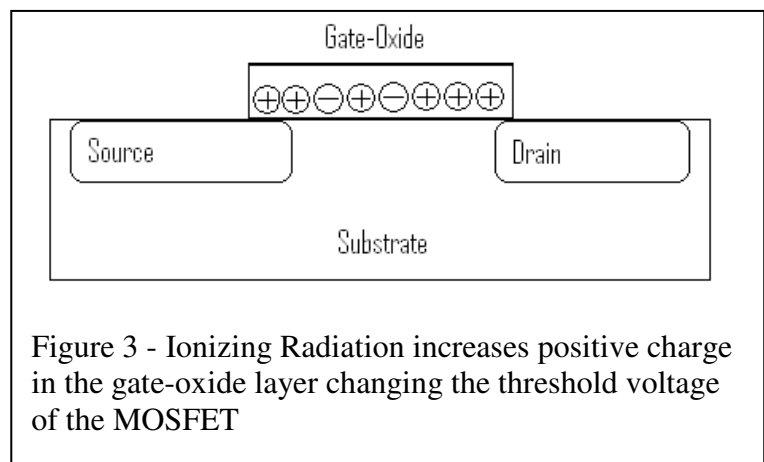
Figure 2 – The wireless dosimeter reader produces a wave that induces a current in the dosimeter and receives the dosimeter's measurements.

circuitry then reads the MOSFETs and uses the antenna to relay this information back to the reader by modulating the incident field.

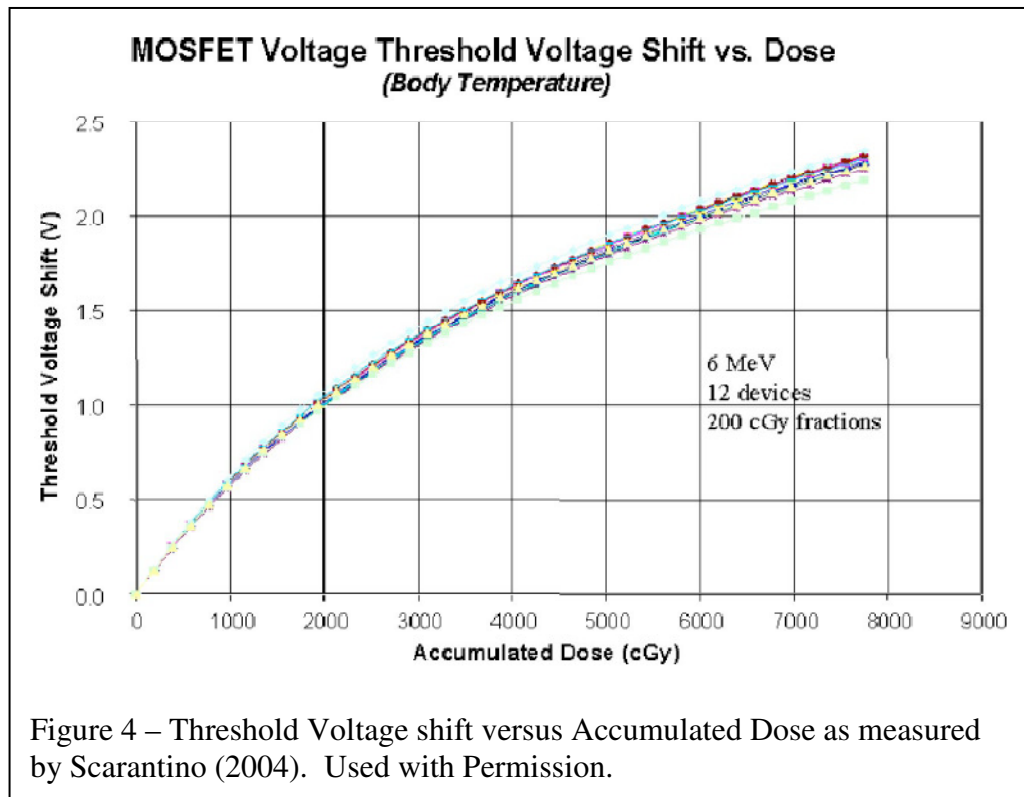
The original dosimeter designed by Sichel was 3mm in diameter and 25mm in length and contained a single MOSFET. Since then, the dosimeter has been redesigned to be smaller and now contains two MOSFETs, whose results are averaged to improve accuracy. The current dosimeter (Figure 1) manufactured by Sichel Technologies is 2.1mm in diameter, 20mm in length and contains two MOSFETs. This new smaller model was used for all data in this thesis. Literature that was based upon the original model will be noted and commented on for perspective, but since all dosimeters used in this thesis were of the new 20mm length variety, comparisons in dosimeter characteristics between this thesis and previous publications will be limited to those publications involving the new 20mm dosimeter.

MOSFET Dosimetry

A MOSFET, as the name states, is a transistor. An oxide insulated gate electrode lies between two electric contacts called a source and a drain (Figure 3). When the gate-oxide has no voltage, no current can flow from the source to the drain. When the gate-oxide is supplied with the necessary amount of voltage (commonly called the threshold voltage), the MOSFET “turns on” and allows current to flow between the source and the drain.



MOSFETs can be used to measure radiation because the threshold voltage necessary to allow current to flow between the source and the drain increases with increasing radiation exposure to the gate-oxide. When radiation is incident upon the MOSFET, it ionizes particles in the gate-oxide separating electrons from molecules. The positively ionized molecule is commonly referred to as a “hole”, because an electron has left the molecule leaving a hole behind. Since the electrons can move more freely than the holes, some holes become trapped in the gate-oxide. These holes are positively charged and therefore increase the threshold voltage necessary to allow current to flow between the source and the drain. The threshold voltage therefore increases as increasing amounts of ionizing radiation increase the number of holes trapped in the gate-oxide. Since the MOSFET is permanently changed by exposure to radiation, it should be considered a cumulative dosimeter. Converting the threshold voltage to dose therefore requires knowing not only the increase in threshold voltage after an exposure, but also the total amount of dose the dosimeter has received. The relationship between voltage shift and dose for the MOSFETs used in the DVS dosimeters for this project is shown in Figure 4 as was measured by the dosimeter’s manufacturer (Scarantino 2004). Since the relationship between voltage and dose is non-linear, the manufacturer supplies a calibration curve for each dosimeter that relates the threshold voltage shift to the accumulated dose.



MOSFET Fading Effect

Over time, some of the holes in the gate-oxide can recombine with electrons reducing the threshold voltage shift necessary to power on the MOSFET. This fading effect must be taken into account when using a MOSFET dosimeter. To overcome this problem, the DVS system was designed to require a pre-irradiation and post-irradiation voltage measurement. Since the time between pre- and post- readings is small, the manufacturer determined empirically that the fade effect would not hinder the accuracy of the dosimeter provided the pre- and post-dose measurements were taken within 30 minutes of each other.

Previous Work with the DVS Dosimeter (original 25mm dosimeter)

The initial study with the DVS dosimeter (original 25mm version) was performed in canines at North Carolina State University - College of Veterinary

Medicine (Scarantino 2004). The publication also reported characteristics of the dosimeter as tested in a phantom and water tank. The dosimeter was noted to have a temperature dependence of “as much as 8 – 20 cGy per degree C (greater variation with more accumulated dose)” (Scarantino 2004). When implanted in a patient, this temperature dependence would be a small source of error, if any, since body temperature is fairly consistent (demonstrated in the paper by placing the canines outside in the cold for 30 minutes and then re-testing showing no change for a 2.5cm deep dosimeter, but a dosimeter between 0.5 and 1.0cm deep showed a slight variation). This temperature dependence is, however, a significant issue for *in vitro* testing, requiring that the DVS dosimeters be temperature controlled in all phantoms and water tanks. The energy dependence of the dosimeter was performed at “6 and 18 MeV [*sic*]” and found to be less than 1.0% (Scarantino 2004). The rotational angular dependence of the dosimeter (i.e. the beam is perpendicular to the long cylindrical axis of the dosimeter and the dosimeter is rotated so that the beam is hitting different sides of the MOSFETs in the dosimeter) was found to be $\pm 1.3\%$. The longitudinal angular dependence of the dosimeter (i.e. the beam is rotated along the long cylindrical axis of the dosimeter so that, for example, at a 270° rotation, the beam passes through the antenna and circuitry before hitting the MOSFET) was not reported and instead it was stated that beams parallel to the cylinder axis would be problematic and therefore surgeons had been instructed to implant the dosimeter so that it would be parallel to the body’s axis. The fade of the dosimeter was reported as $<2\%$ over 20 minutes. The precision of the dosimeter was reported as 3.5cGy due to using a 12-bit analog-to-digital converter. The

author stated that the new dosimeter would have a 14-bit converter increasing the precision of the dosimeter to 0.8cGy (Scarantino 2004).

A pilot study to test the safety and utility of the dosimeter (original 25mm dosimeter) was performed at Rex Healthcare (Raleigh, NC) and Duke University School of Medicine (Durham, NC) with implantation in “3 patients with lung cancer, 3 patients with prostate cancer, 3 patients with rectal cancer, and 1 patient with a sarcoma in the lower extremity” (Scarantino 2005). The dosimeter characteristics section focused on the angular dependence of the dosimeter and stated that extensive testing of the dose isotropy had been performed on the longitudinal axis and had found that “the results hold as long as the angle of incidence is more than 30 degrees from the axis of the device” (Scarantino 2005). If we define 270° as a beam which would go through the antenna and circuitry of the dosimeter before reaching the MOSFET, 0° as a beam perpendicular to the cylindrical axis and 90° as a beam which would go perpendicularly through the MOSFET side of the dosimeter first, then the authors appear to be stating that the longitudinal angular dependence of the dosimeter is not an issue between 300° and 60° . It is unclear what “the results hold” means in terms of an error value, but the author states that combining all of the errors gives the dosimeter an absolute accuracy value of 3.5% (1 standard deviation).

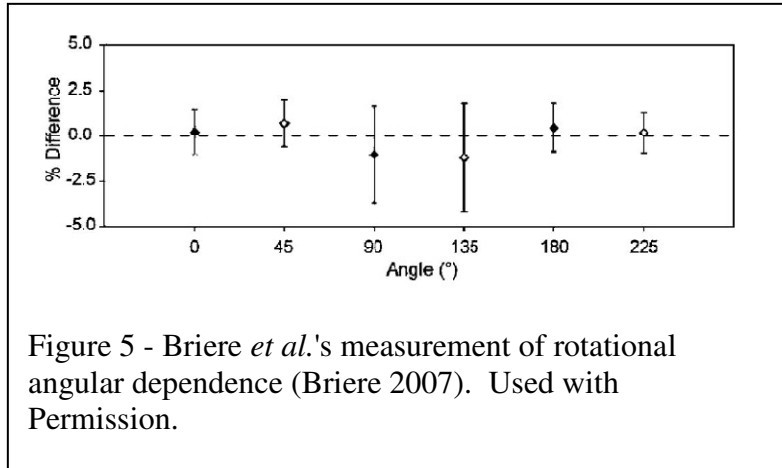
Three additional papers were published testing the original 25mm dosimeter, all three focusing primarily on the reproducibility of readings (Beddar 2005, Briere 2005, Black 2005). The first, performed at this institution (The University of Texas MD Anderson Cancer Center, Houston, TX), used a Cobalt-60 unit to test the reproducibility of the MOSFET threshold voltage and found a dose reproducibility within 5% or better,

2% or better with a better temperature controlled environment (Beddar 2005). The second publication, also performed at this institution, tested the reproducibility of the dosimeter *dose* reading, which takes into account the reproducibility of not only the MOSFET threshold voltage shift, but also how well the manufacturer's calibration curve related the voltage shift to an accurate dose value (Briere 2005). The dose per fraction was varied from 100cGy/Fx to 400cGy/Fx and it was found that reproducibility varied from a standard deviation of 3.6% for the 100cGy/Fx reading to roughly 2% for the 200 and 400cGy/Fx readings (Briere 2005). The third publication combined an *in vitro* study of the dosimeter in a phantom with an *in vivo* study of the dosimeter implanted in 18 patients and found that *in vitro* errors within $\pm 5\%$ are achievable, but that *in vivo* measurements frequently exceeded these levels (Black 2005).

Two additional papers using the original DVS dosimeter were published, both reporting strictly *in vivo* results (Beyer 2007, Scarantino 2008). The dosimeters were clinically tested in prostate (Beyer 2007) and breast and prostate (Scarantino 2008) disease sites. Both papers found that the doses could vary significantly from planned. Both Beyer and Scarantino mention in the introduction that a new smaller version of the DVS dosimeter is now available. Also, in the conclusions both papers suggest that the marker could be used for IGRT treatments since it is “visible in kV, CT, and ultrasound images” (Beyer 2007).

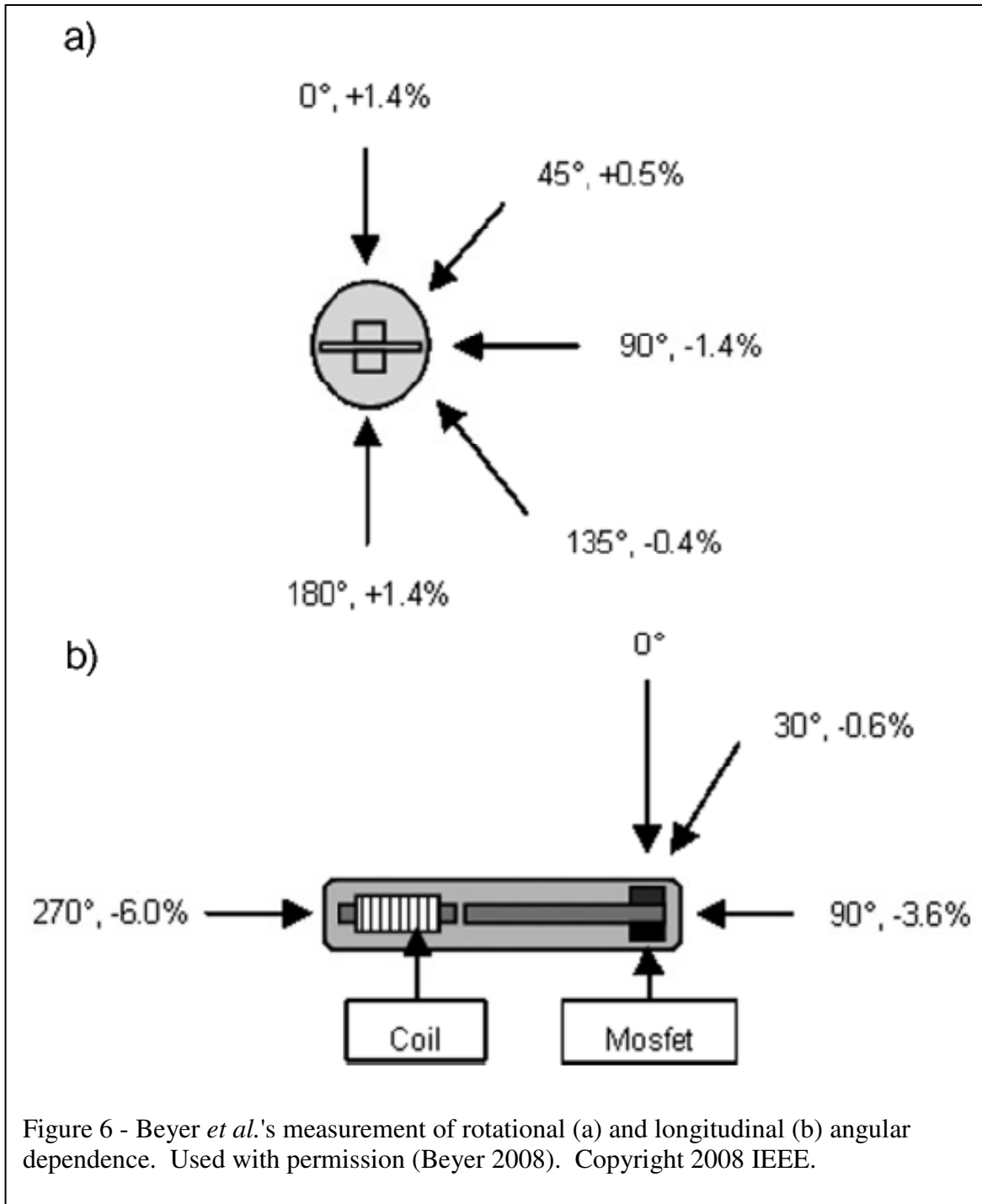
Previous Work with the DVS Dosimeter (new 20mm dosimeter)

The first paper evaluating the new smaller dosimeter design tested the dose per fraction and rotational angular dependence (Briere 2007). Briere *et al.* used the manufacturer's dose calibration curve to record readings at rotational angles of 0, 45, 90, 135, 180 and 225. Two dosimeters per angle were used and each reading was repeated three



times. The results are shown in Figure 5. The results are relative to the dosimeter's mean value and “[do] not vary by more than 1.2%” (Briere 2007).

A more complete characterization of the DVS dosimeter was published by Beyer *et al.* and included information on the dosimeter's energy dependence as well as angular dependence in both the rotational and longitudinal directions (Beyer 2008). Beyer *et al.* found that 15MV photons read 0.5% higher than 6MV photons. The angular dependence results are shown in Figure 6.



DVS Dosimeter (new 20mm dosimeter) in other radiotherapy treatment modalities

The DVS dosimeter has also been tested in brachytherapy (Fagerstrom 2008) and with a Cyberknife® system (Accuray Inc., Sunnyvale, CA) (Scalchi 2010). The Cyberknife® paper verified that the DVS dosimeter could be used in Cyberknife® treatment without additional corrections (Scalchi 2010). No characteristics relevant to this work were investigated.

The brachytherapy paper found a “clear difference in detector sensitivity... for ^{60}Co and ^{192}Ir energies”, which could not be linearly corrected for (Fagerstrom 2008). This paper also tested the rotational angular dependence and found an average variation of “less than 1.5% for each angle, showing little dosimeter dependence on incident rotational angle” (Figure 7) (Fagerstrom 2008). Fagerstrom *et al.* also tested the longitudinal angular dependence (Figure 8) and found a -16% angular dependence through the antenna coil for the ^{192}Ir . It is important to note that this paper ignored the previously established angle definitions in favor of a completely opposite definition. Therefore, 90° is through the antenna coil, whereas all other papers including this thesis, define 270° as through the antenna coil.

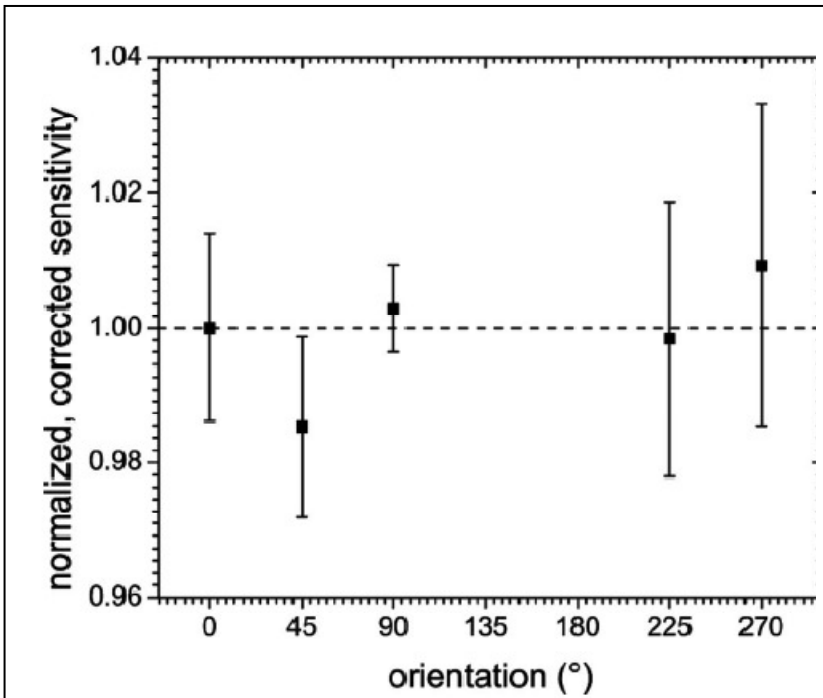


Figure 7 - Fagerstrom *et al.*'s rotational angular dependence results (Fagerstrom 2008)

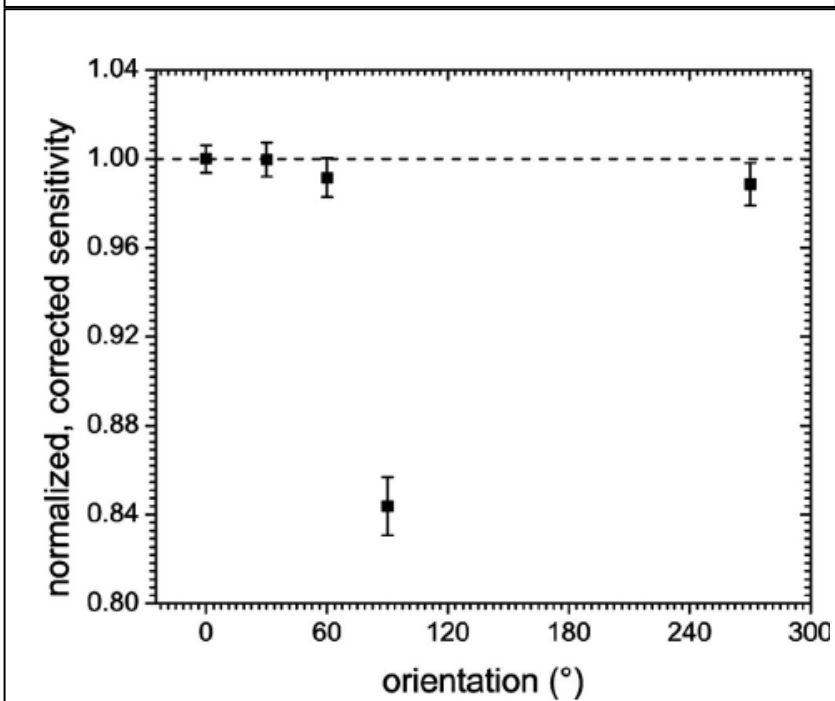


Figure 8 - Fagerstrom *et al.*'s longitudinal angular dependence (Fagerstrom 2008). Used with Permission.

Using the DVS dosimeter as a fiducial marker

After much speculation that the DVS dosimeter could be used as a fiducial marker, one paper tested the assumption (Kry 2009). Of course, since the commercially available dosimeter can only be seen with kV-level imaging, a kV imager was used. Kry *et al.* found that the detectors were easily visualized at kV levels and that displacements were recognized by the localization software to within 0.1cm (Kry 2009).

METHODS AND MATERIALS

Prototype Dosimeters

The manufacturer, Sicel Technologies, had several ideas for incorporating a gold marker into their design. Therefore, it was necessary to test some different methods

before deciding on a design

with which to test the

dosimetry. The

manufacturer proposed

adding a gold sleeve to the

antenna part of the dosimeter

(Figure 9B), adding solid

gold to both ends of the

dosimeter (not shown), or

adding gold wire to wrap

around the antenna assembly

(Figure 9C). After

attempting fabrication, the

company determined that

redesigning the dosimeter in

order to add a marker to both

sides was infeasible. It

therefore abandoned the dual-marker design and sent only the gold wire and gold sleeve design.



Dosimeter A : Standard dosimeter.



Dosimeter B : Gold Sleeve installed over end of antenna ferrite core



Dosimeter C : Wound gold wire marker installed over end of antenna ferrite core.

Figure 9 - Prototype Dosimeters Standard (A) Gold Sleeve (B) and Wire Wrapped (C)

Imaging – Prototype Visualization Study

These prototypes, along with a commercially available dosimeter, clinically used 0.8mm x 3.0mm and 1.2mm x 3.0mm

cylinder gold markers (CIVCO Medical Solutions, Kalona, IA) and a prototype made by Dr. Salehpour (one of the old 25mm dosimeters, broken open and with gold melted on the inside of one end) were imaged in a Rando anthropomorphic phantom (The Phantom Laboratory, Salem, NY) as shown in Figure 10. The phantom

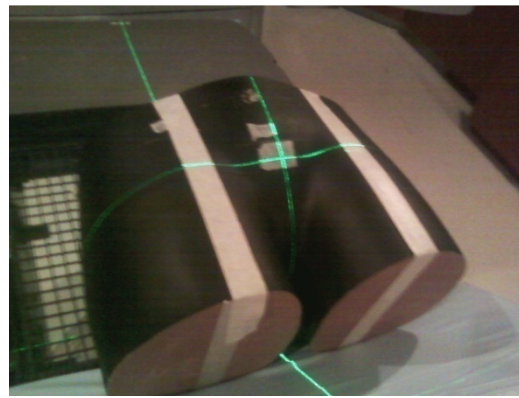


Figure 10 - Pelvic section of Rando phantom used for preliminary imaging study

and fiducials were imaged using the On Board Imager® (OBI; Varian Medical Systems, Palo Alto, CA) on a linear accelerator (linac) clinically used for IGRT treatment. Anteroposterior (AP) and lateral images were taken at both MV and kV levels. Also, cone beam CT (CBCT) was taken using the OBI. Clinically used imaging techniques were used including 2MU for the AP MV image, 5MU for the lateral MV image, 84kVp, 10 mAs for the AP kV image and 105kVp, 80mAs for the lateral kV image. Since this was a preliminary study, all markers were placed in the phantom at the same time to avoid the considerable time needed to open the phantom, replace a fiducial marker, set up and re-image. Therefore, after deciding upon a dosimeter design, the imaging part was repeated under more controlled conditions. To provide a quantifiable visualization measurement, the difference in pixel value between the dosimeters and a nearby background was calculated on the MV AP image. The difference was calculated with a

freely available DICOM image viewer (ImageJ v1.43, U.S. National Institute of Health, Bethesda, MD). To calculate the difference, the mean pixel value of a region of interest (ROI) contained within the marker part of each dosimeter was compared to an ROI of the same size outside, but close to each dosimeter. The mean pixel value of the background ROI was subtracted from the mean pixel value of the marker to determine the mean pixel value difference between the two.

Modified Dosimeter

Based upon the preliminary study, the wire-wrapped dosimeter design was chosen (see Results & Discussion section). The modified dosimeter (Figure 11) is slightly longer than the commercially available dosimeter since fabrication of the modified dosimeter required re-sealing of the commercially available dosimeter. The additional length also made it impossible for the modified dosimeter to fit into the manufacturer's calibration apparatus,

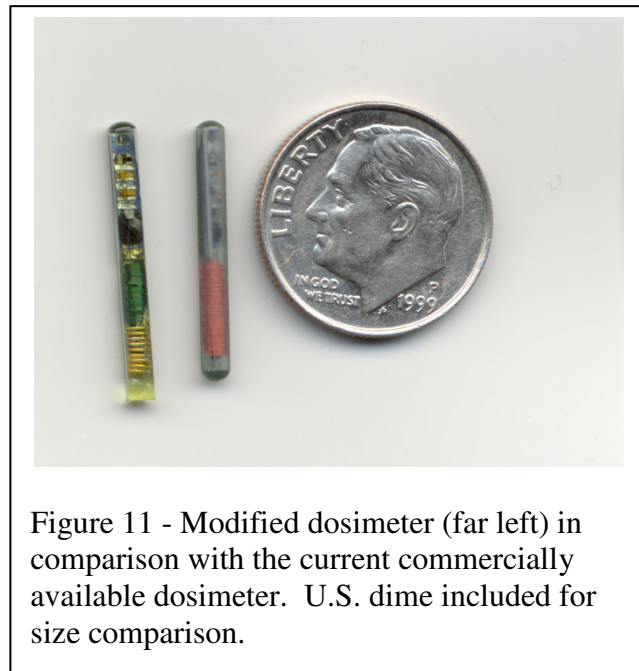


Figure 11 - Modified dosimeter (far left) in comparison with the current commercially available dosimeter. U.S. dime included for size comparison.

which is used to form the calibration curve necessary to convert the threshold voltage shift of the MOSFETs into a dose value. Therefore, acquisition of the data required a “self-calibration” method as described later in the “Data Acquisition – Compensating for the Calibration Curve” section.

Imaging – Controlled Study

After choosing to proceed with the wire-wrapped model dosimeter, the imaging part of the study was repeated placing each item to be imaged at the same position in the phantom. Since the provided wire-wrapped models varied slightly from the first provided prototype, the new model was used for this imaging study. The Rando anthropomorphic phantom was again used (Figure 12), adding the compression device in an attempt to reduce streaking artifacts between the

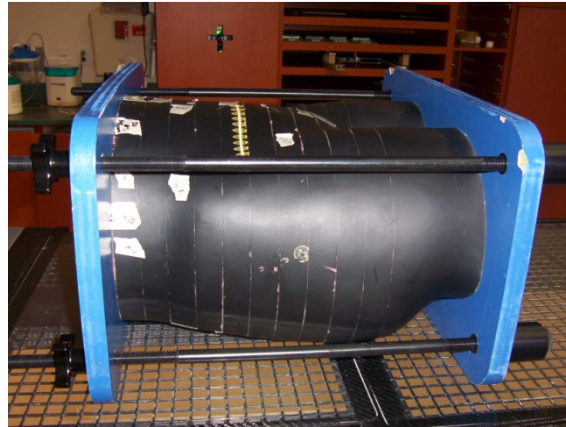


Figure 12 - Pelvic section of Rando phantom used for controlled imaging study

slices. The commercial dosimeter, modified dosimeter (wire wrapped model), a clinically used 0.8mm x 3.0mm cylinder gold fiducial marker (CIVCO Medical Solutions, Kalona, IA) and a clinically used carbon dumbbell fiducial marker (Carbon Medical Technologies, St.Paul, MN) were imaged one at a time in the same location. The location was chosen to be near the pubic symphysis of the Rando phantom since the dosimeters have been clinically tested for prostate disease sites and since IGRT is commonly used in the treatment of prostate cancer.

A line profile of the dosimeters and markers showing pixel value versus position was created in a freely available DICOM image viewer (ImageJ v1.43, U.S. National Institute of Health, Bethesda, MD). The line profiles were used as a quantifiable way of assessing visibility.

Wireless Reader

The dosimeters are read with a wireless reader supplied by the manufacturer (Figure 2). This reader consists of a wand and base computer system. This computer

system is networked to an institution's database. Patients are loaded into the database and the dosimeters assigned to each patient, as well as the predicted dose to each dosimeter, are recorded. The dosimeters are assigned to each patient using a manufacturer-supplied bar code (Figure 13). This bar code contains the dosimeter identification information and supplies the coefficients of the calibration curve needed to convert the dosimeter's voltage reading into a dose. When a dosimeter needs to be read, the patient to

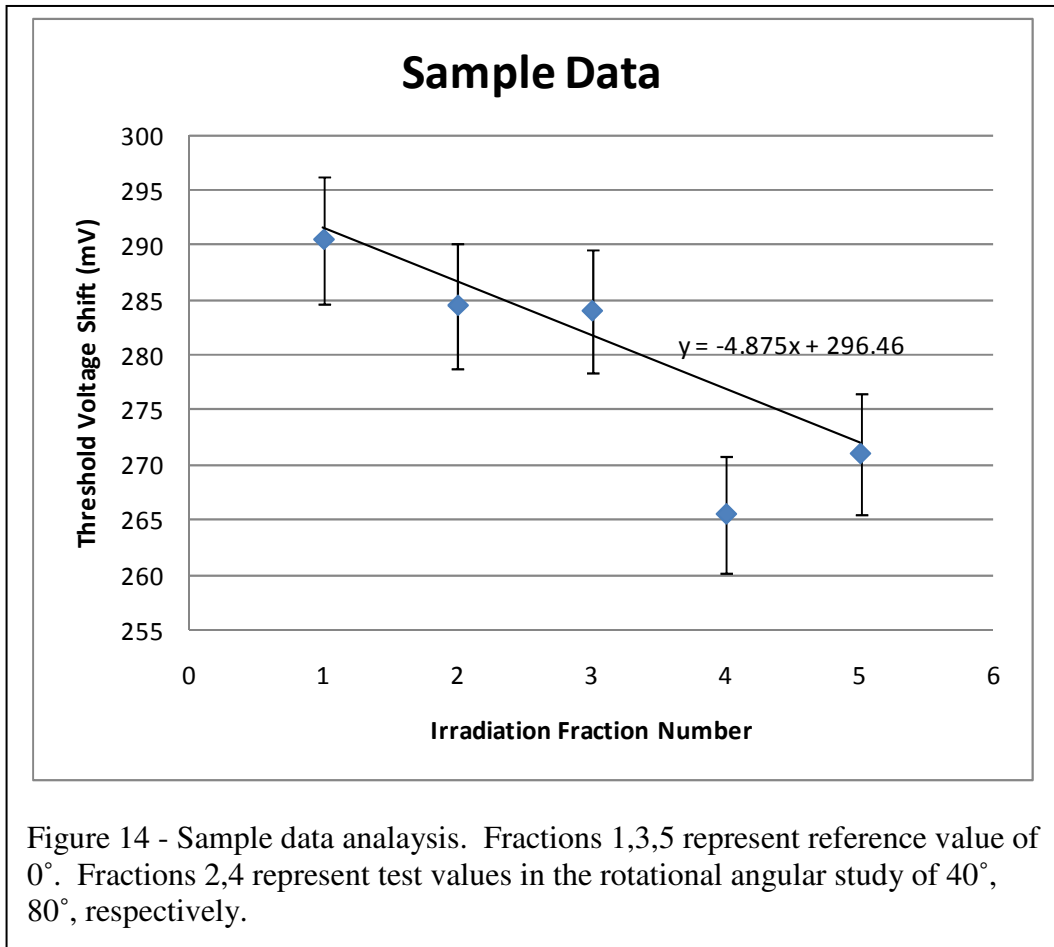


Figure 13 - Bar Code Reader (top) and sample bar code (bottom)

be read is selected using the reader's base display. Then, the wand is placed near the patient and a high voltage supply generates an electromagnetic wave. This wave powers the dosimeters through their antenna. As the dosimeter is powered, it uses the antenna to modulate the incident electromagnetic wave, which sends back the threshold voltage read on each of the two MOSFETs. The wand acts as both transmitter and receiver of the electromagnetic waves. The reader's base station converts the threshold voltage read by the MOSFETs into a dose value using the manufacturer's supplied calibration curve.

Data Acquisition – Compensating for the Calibration Curve

As mentioned earlier, the modified dosimeters were too long to be calibrated by the manufacturer, as the commercially available dosimeters would be. In order to relate the threshold voltage shift in the MOSFETs to a known dose, it was necessary to acquire the data in a certain fashion so that our own calibration curve could be created. The procedure described below was suggested by the manufacturer, Sichel Technologies, and had been used for studies performed by the manufacturer and in previous publications with the dosimeter (e.g. Beyer 2008). The procedure involves taken a known reference value in between each desired measurement. Then, a linear fit (which acts as the calibration curve) is applied to the reference values and the measured values are compared to their expected position on this line. For example, in the rotational angular dependence tests, 0° was chosen as the reference value. Data were taken in the order 0° , 40° , 0° , 80° , 0° , etc. This analysis is shown graphically in Figure 14.



One major advantage of this procedure is that multiple measurements can be taken in a single session, rather than separating measurements by 24 hours. (If using the calibration curve, readings must be separated since the curve assumes a clinical treatment schedule and therefore compensates for the fading effect that would occur over the typical 24-hour period between irradiation fractions.) To ensure the accuracy of this procedure, data were taken under strict time controls. A stopwatch was used to measure that the time between pre- and post- irradiation readings, time between measurements, and time of irradiation were the same for the entire series of a test procedure. These controls were necessary to ensure that the time-dependent fading effect did not add any uncertainty into the data.

Read Range Study

There was concern upon modifying the dosimeters that the depth at which they would be able to be read might be compromised. A dosimeter that is unable to be read is useless. Therefore, the read range of both the commercial and modified dosimeters was tested for comparison. Three dosimeters were placed in a holder designed for use in the energy dependence study (Figure 15). This holder was placed inside a water tank with the

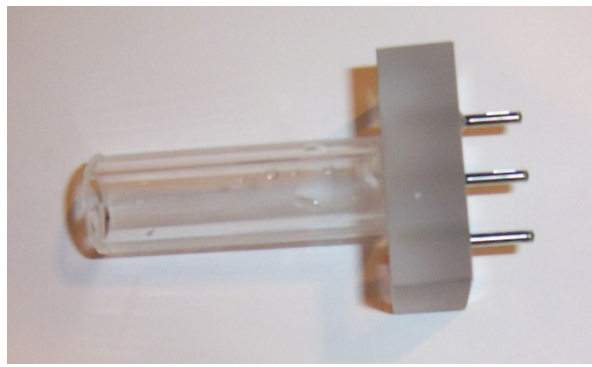


Figure 15 - Dosimeter holder with three DVS dosimeters.

wireless reader placed as close as possible to the side of the tank. The distance of the dosimeters from the reader was measured using a measuring tape and the distance was increased by 1cm until the reader was no longer able to read the voltage from one or more of the three dosimeters. The greatest distance at which all three dosimeters could be read was recorded as the read range.

Energy Dependence Study

The energy dependence of the dosimeters at 6MV and 15MV photon energies was investigated using a water-tank (Figure 17) of the type typically used for Task Group 51 calculations (TG51; Almond 1999). Since the MOSFETs have some temperature dependence which, though not an issue in the temperature regulated body, can be an issue in *in vitro* testing, the water was temperature controlled to 37° C and a small circulating pump was placed in the tank to ensure that the heated water was evenly distributed throughout the tank. A Farmer-type ion chamber (PTW 30013; PTW-New York Corporation, Hicksville, NY) was placed in a depth-control apparatus in the water tank. The depth of the ion chamber was

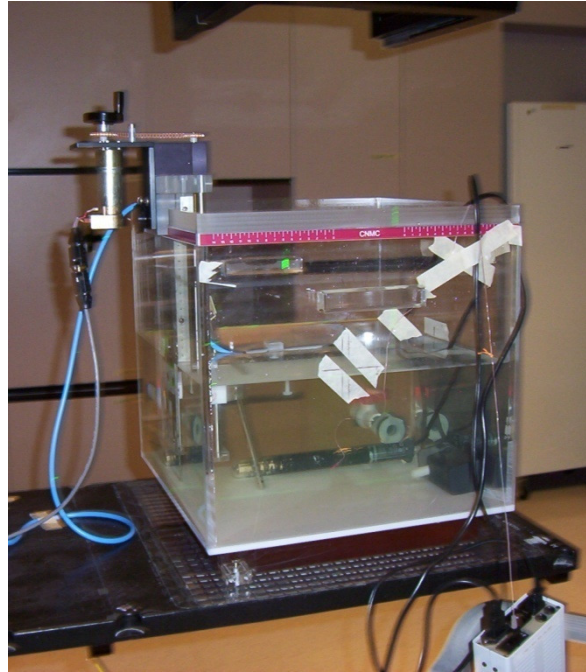


Figure 17 – The water tank is shown with heater apparatus and circulating pump.

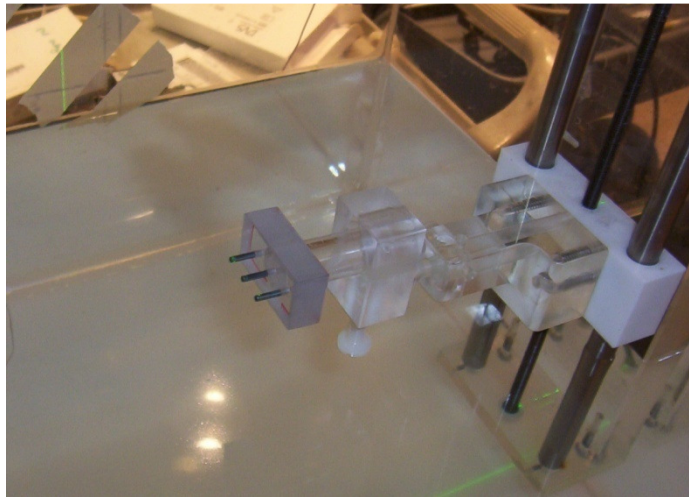


Figure 16 - Dosimeter holder in water tank. The tube end of the dosimeter holder is the same size as the ionization chamber used in the tank allowing the MOSFET readings to be compared with absolute dose measurements.

adjusted for each energy until d_{\max} was found. The exposure at this depth was converted into absolute dose according to TG51 protocol. A custom designed holder was manufactured to hold three DVS dosimeters in the same apparatus as the ion chamber (Figure 15, Figure 16). The center dosimeter was placed in the center of the beam with a dosimeter 1cm away on either side. After using the ion chamber to find d_{\max} and calculate the dose at that point (d_{\max} includes the adjustment for the active volume of the ion chamber by shifting by $0.6 r_{\text{cav}}$ according to TG-51 protocol), the ion chamber was removed and replaced with this apparatus. Readings for 6MV and 15MV photon energies were taken at their respective d_{\max} 's. The procedure was repeated three times with three dosimeters each time for a total of nine readings. 6MV photons were chosen as the reference value. The readings from the dosimeters were corrected for any difference in the expected dose as calculated by the ion chamber. Both the modified and commercial dosimeters were tested with this procedure for comparison.

Angular Dependence Temperature Control Apparatus

As mentioned previously, since the MOSFETs are temperature sensitive, it was necessary to control the temperature of the dosimeters for *in vitro* testing. This was accomplished using tubing connected to a tank of heated water (Figure 18). A small pump circulates the water through a series of tubing which runs

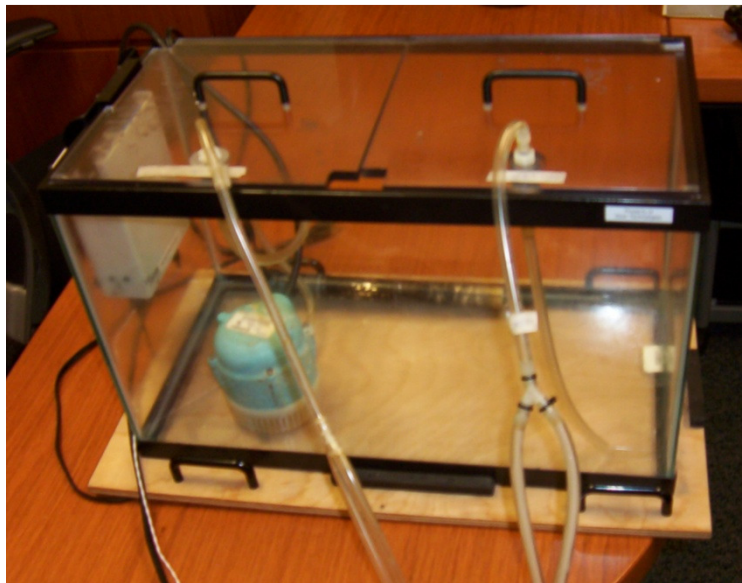


Figure 18 – Temperature controlled water supply flowed through all phantoms used in this study to keep the MOSFETs at 37° C.

through the angular dependence phantom. A thermistor on the tubing is connected to a controller (CN9500 CSC32, Omega Engineering, Inc., Stamford, CT), which powers on an aquarium heater. The controller was set to heat the water to 37° C. The temperature was verified using independent thermistors connected to an electronic thermometer (800023, Sper Scientific, Scottsdale, AZ).

Angle Definition

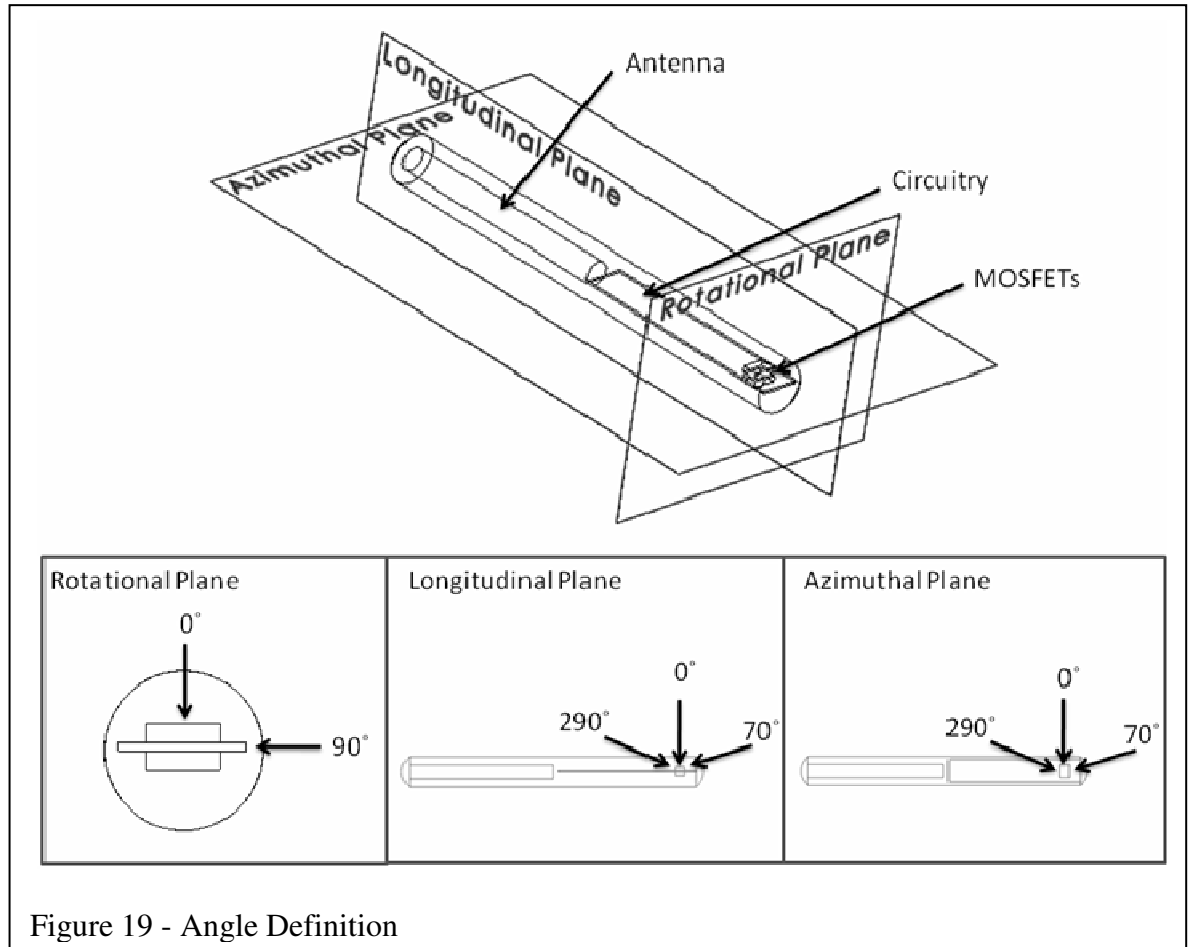


Figure 19 - Angle Definition

The angular dependence of the dosimeter from a wide range of angles was tested. To aid in understanding this data, it is important to define the angles in various planes. As is shown in Figure 19, rotational angles are defined as angles around the short axis of the dosimeter. The longitudinal angles are angles across the long axis of the dosimeter at a 0° rotation. All longitudinal angles are therefore incident on the back of the circuitry substrate. Azimuthal angles are longitudinal angles at a 90° rotation. Azimuthal angles are therefore incident on the side of the circuitry substrate.

Angular Dependence Study

The angular dependence study was performed in a custom designed spherical phantom. The phantom holds one dosimeter at the center of the sphere, enabling beams from a wide range of angles to pass through the same amount of material before being incident on the dosimeter. The insert within the phantom allows the dosimeter to be rotated through various rotational angles. The insert is also fitted with tubing apparatus to enable heated water to flow through the phantom, ensuring that the dosimeter is kept at a constant temperature. A CT scan of the phantom was obtained (GE Lightspeed16; GE Healthcare, Waukesha, WI) and the dose from beams at different gantry angles was calculated using a treatment planning system (Pinnacle v8.0m, Philips



Figure 20 - Spherical Phantom (top) close-up of insert (middle; dosimeter identified with dashed circle) and close-up of side of phantom showing how insert can be rotated (bottom)

Healthcare, Andover, MA). Based upon the dose calculations of the treatment planning system, it was found that beams incident in the longitudinal direction on to the dosimeter from 290° - 70° resulted in doses to the sensitive part of the dosimeter to within 0.5% of each other. Longitudinal angles more extreme than this began to be attenuated by the tubing and holder apparatus and therefore resulted in lower doses than the other angles. The study was therefore limited to longitudinal angles between 290° and 70° . The longitudinal angles 290° , 310° , 330° , 350° , 0° , 10° , 30° , 50° , and 70° were chosen to be measured. For the rotational direction, it was desired that angles from all directions be taken so angles at every 40° were chosen. It was also desired to compare these results to previously published work, so angles at 90° , 180° and 270° were also chosen. The rotational angles tested were therefore 0° , 40° , 80° , 90° , 120° , 160° , 180° , 200° , 240° , 270° , 280° and 320° . After discovering that the 90° rotational angle under responded when compared to the 0° angle, it was decided to also test the longitudinal dependence of the dosimeter when it had been rotated 90° (i.e. the radiation beam is incident on the side of the circuitry board) to see how it compared to the longitudinal dependence at 0° (i.e. the radiation beam is incident on the face of the circuitry board). This so-called “azimuthal” dependence was tested at the same angles as the longitudinal dependence of 290° , 310° , 330° , 350° , 0° , 10° , 30° , 50° , and 70° . Since no data had been published that covered such a comprehensive set of angles, it was necessary to perform the procedure on both the modified and commercial dosimeters for comparison. Each angle was tested with three different dosimeters of each type.

RESULTS AND DISCUSSION

Imaging – Prototype Visualization Study

The images acquired for this study are shown in the figures below. The dosimeters are labeled according to the legend in Table 1, which also shows the contrast between the imaged marker or dosimeter and a nearby background in terms of pixel difference. The kV AP view of the dosimeters is shown in Figure 21. The MV AP view is shown in Figure 22. The kV lateral view is shown in Figure 23. The MV lateral view is shown in Figure 24. The CBCT slices are shown in Figure 25.

Table 1 - Prototype OBI Images Legend		
Label	Dosimeter	Pixel Difference from Background
A	Standard Dosimeter	5
B	Gold Sleeve Modified Dosimeter	34
C	Wire Wrapped Modified Dosimeter	26
D	25mm Dosimeter with Gold Marker	36
E	1.2mm x 3.0mm Gold Marker	35
F	0.8mm x 3.0mm Gold Marker	21

Table 1 - Legend for Prototype Visualization Images and Average Pixel Difference from Background on MV AP image

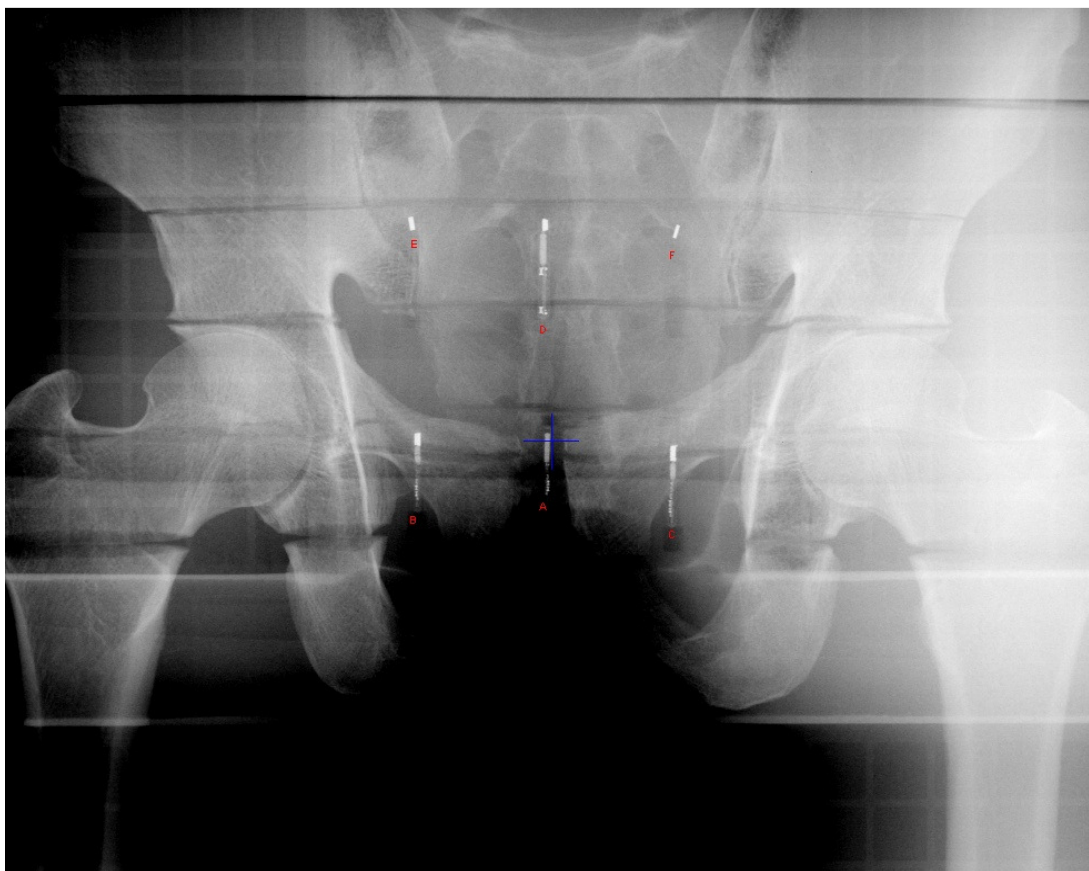


Figure 21 - kV AP View of Prototype Visualization Study. From top left to bottom right: E (1.2mm Gold Marker), D (25mm Dosimeter with Marker), F (0.8mm Gold Marker), B (Gold Sleeve Modified Dosimeter), A (Standard Dosimeter), C (Wire Wrapped Modified Dosimeter)

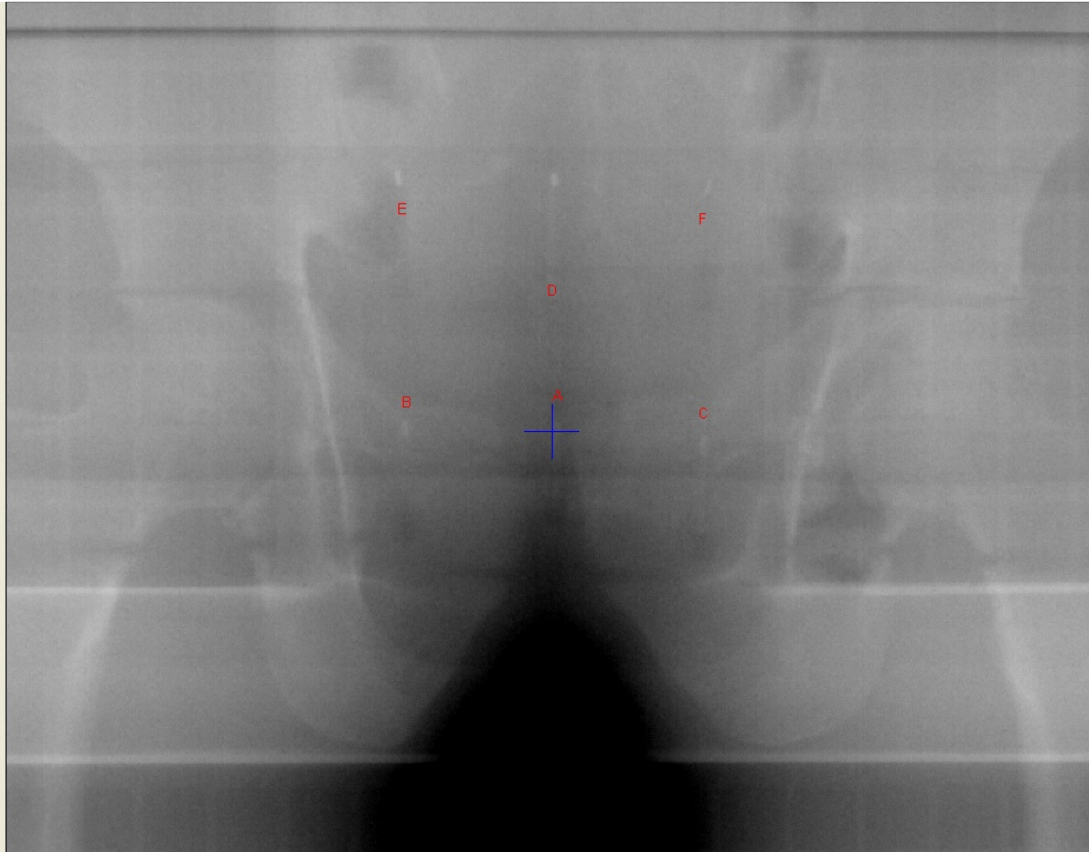


Figure 22 - MV AP View of Prototype Visualization Study. From top left to bottom right: E (1.2mm Gold Marker), D (25mm Dosimeter with Marker), F (0.8mm Gold Marker), B (Gold Sleeve Modified Dosimeter), A (Standard Dosimeter), C (Wire Wrapped Modified Dosimeter)

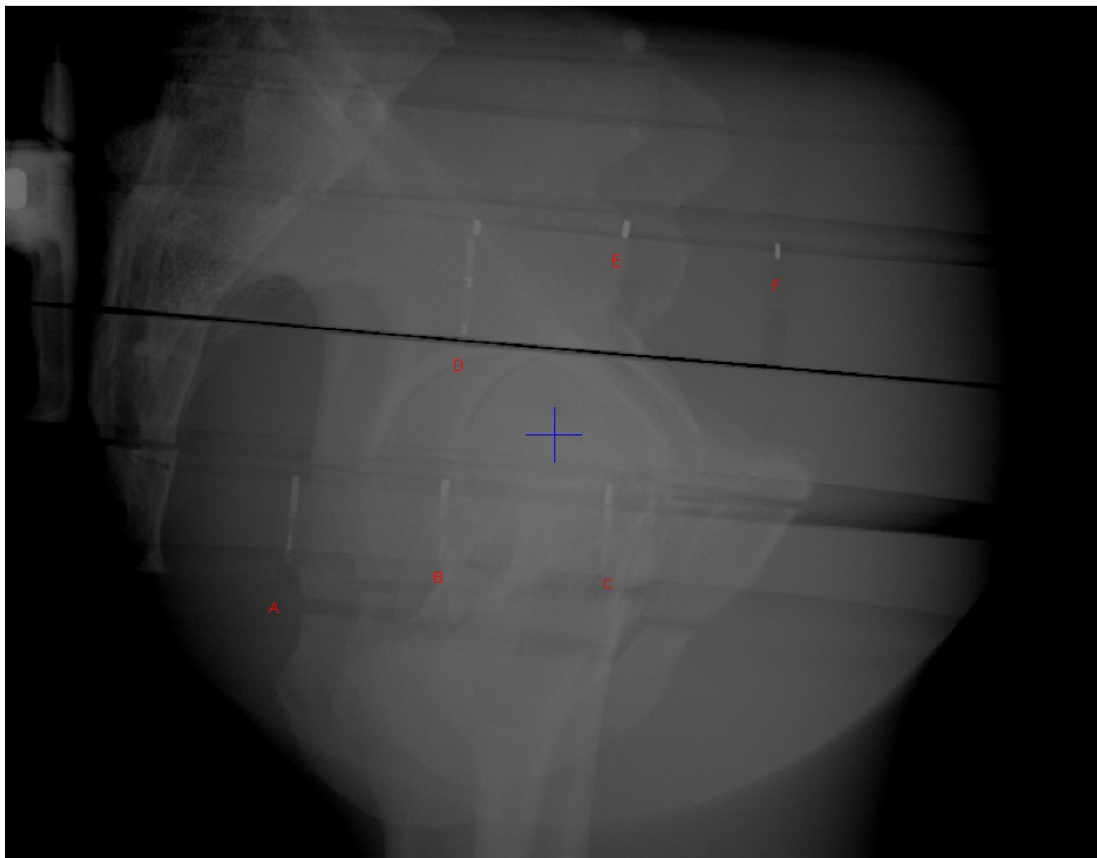


Figure 23 - kV Lateral View of Prototype Visualization Study. From top left to bottom right: D (25mm Dosimeter with Marker), E (1.2mm Gold Marker), F (0.8mm Gold Marker), A (Standard Dosimeter), B (Gold Sleeve Modified Dosimeter), C (Wire Wrapped Modified Dosimeter)

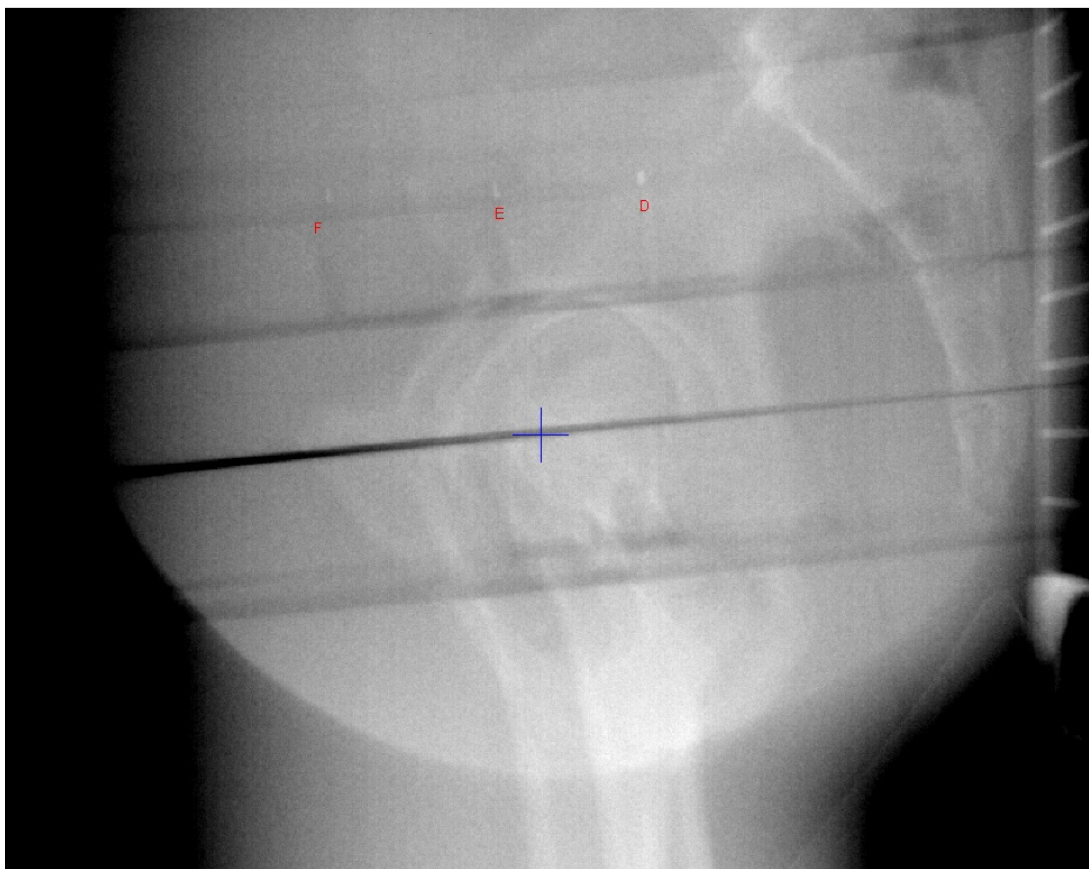


Figure 24 - MV Lateral View of Prototype Visualization Study. From left to right: F (0.8mm Gold Marker), E (1.2mm Gold Marker), D (25mm Dosimeter with Marker). Markers A – C unviewable due to streak

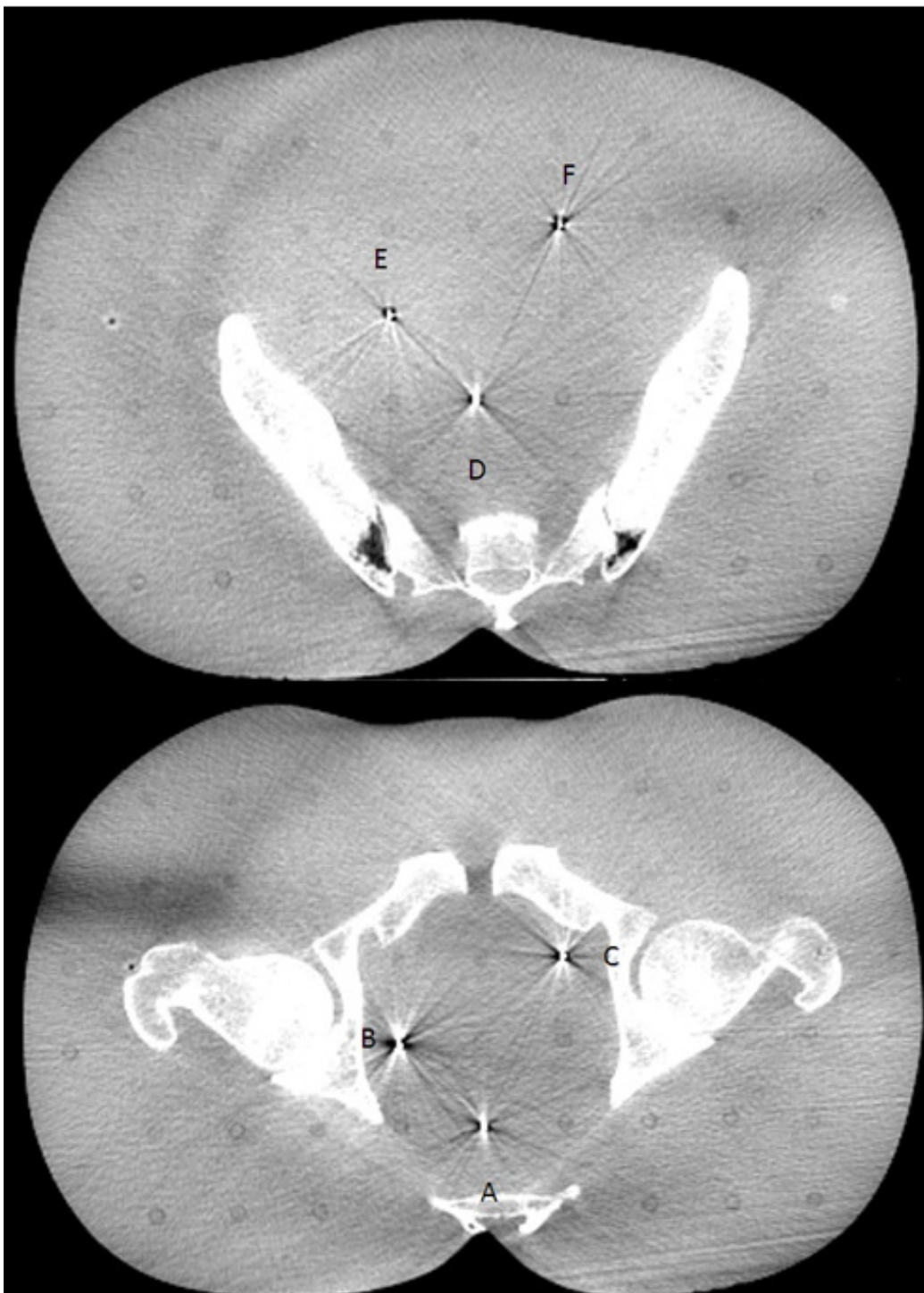


Figure 25 - CBCT Slice of Prototype Visualization Study. Top Image left to right: E (1.2mm Gold Marker), D (25mm Dosimeter with Marker), F (0.8mm Gold Marker). Bottom Image left to right: B (Gold Sleeve Modified Dosimeter), A (Standard Dosimeter), C (Wire Wrapped Modified Dosimeter)

All six tested markers were visible on the kV AP and lateral images and the CBCT, as expected. The MV lateral image (Figure 24) had a streak artifact obscuring markers A, B and C however, the MV AP image (Figure 22) shows that all markers, with the exception of the standard dosimeter, are visible. The standard dosimeter had the lowest difference from background of only 5, making it very difficult to see. The modified dosimeter prototypes were similar in visibility to the commercially available fiducial markers, although the artifacts on the CBCT were significantly higher for the modified dosimeters than for the markers. The artifacts from the modified dosimeters seemed similar to the commercially available dosimeter with the gold sleeve modified dosimeter possibly having more artifacts. The results of this study were reported to the manufacturer. Since both modified dosimeter prototypes were visible on the MV AP image, the next step was to determine the prototype with which to proceed. After some discussion with the manufacturer, it was discovered that the gold sleeve modified dosimeter caused a significant hindrance in the wireless read range of the dosimeter. The gold sleeve induced eddy currents in the antenna assembly, which, in the manufacturer's read range test, reduced the wireless read range from 15cm to 9cm. Therefore, the decision was made to proceed with the wire-wrapped design for dosimetry testing.

Imaging – Controlled Study

Ten wire-wrapped model modified dosimeters were provided for the dosimetry studies. These dosimeters were more carefully manufactured than the prototypes and so were slightly different from the wire-wrapped prototype imaged in the preliminary

study. In addition, the preliminary study did not equally compare the dosimeters since they were all done at a different location in the phantom. Therefore, new images were taken under more controlled conditions and using the same modified dosimeter as would be used for all of the dosimetry tests. The commercial dosimeter, wire-wrapped modified dosimeter, 0.8mm x 3.0mm gold marker, and carbon dumbbell marker were imaged. The kV AP images are shown in Figure 26. The MV AP images are shown in Figure 27 and a closer view of these images is provided in Figure 28. The kV lateral images are shown in Figure 29 and the MV lateral images are shown in Figure 30. The CBCT slices are shown in Figure 31 and Figure 32. Line profiles to provide a quantitative assessment of visualization are shown in Figure 33 and Figure 34.

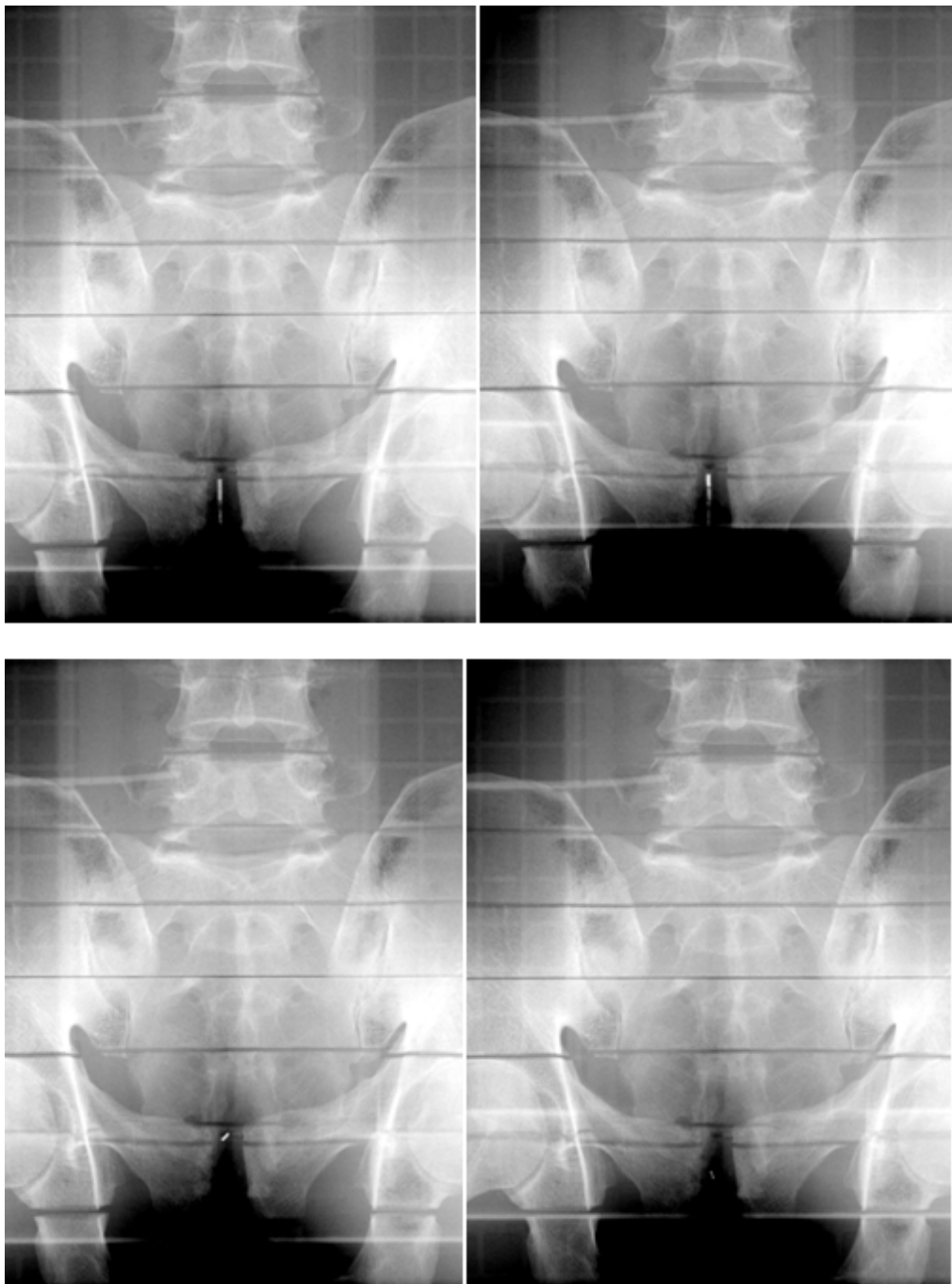


Figure 26 - kV AP images. From top left to bottom right: Commercially Available Dosimeter, Modified Dosimeter, Gold Marker, Carbon Marker

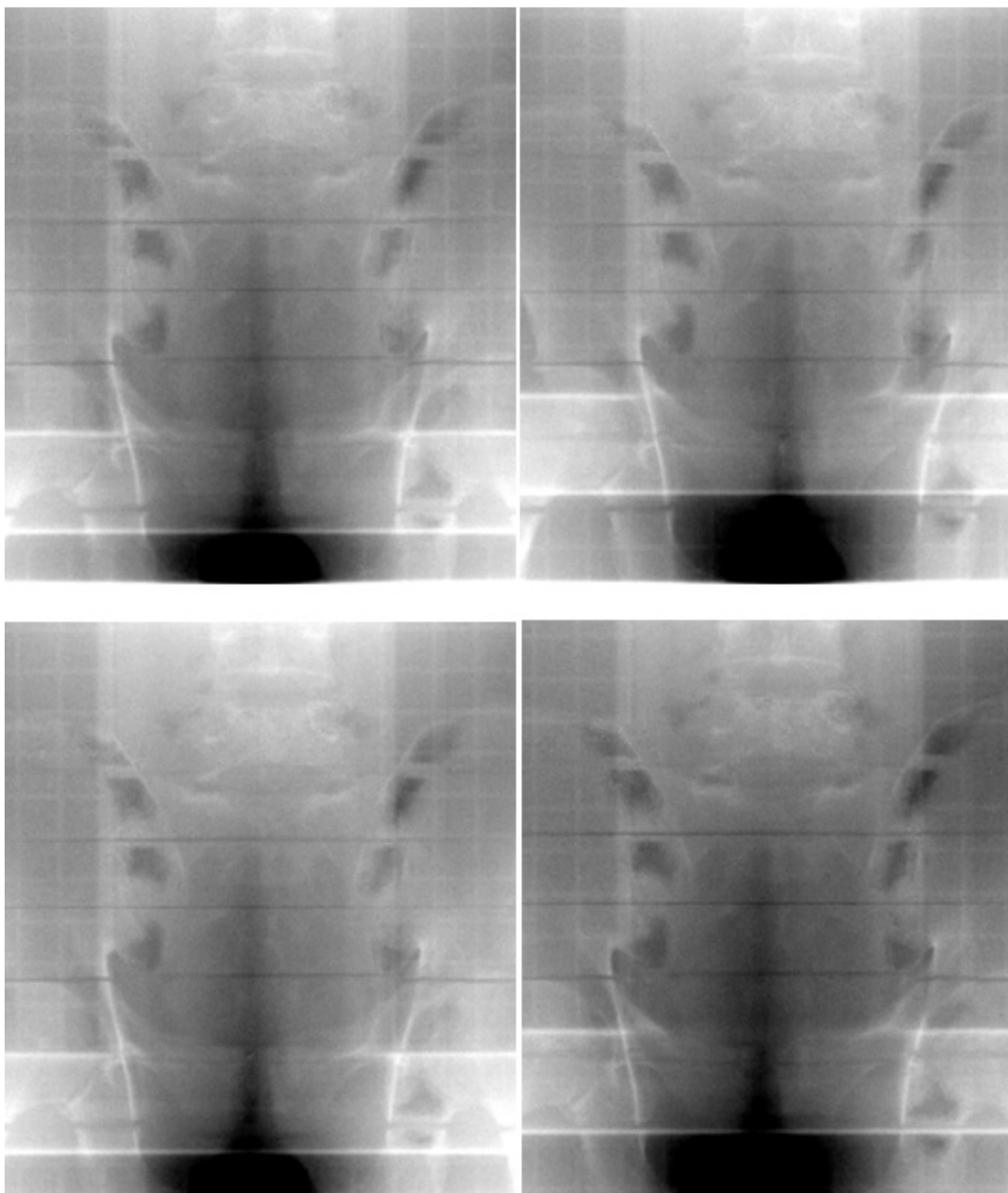


Figure 27 - MV AP images. From top left to bottom right: Commercially Available Dosimeter, Modified Dosimeter, Gold Marker, Carbon Marker

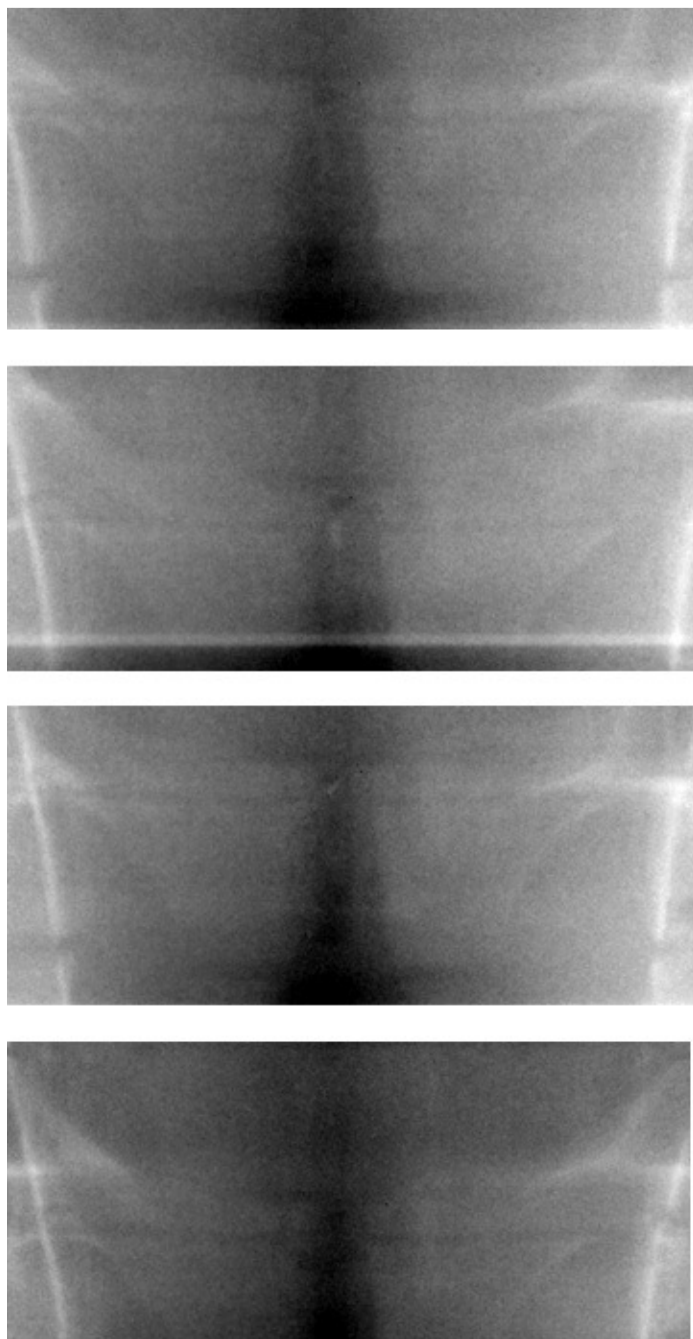


Figure 28 - MV AP images Magnified. From top to bottom: Commercially Available Dosimeter, Modified Dosimeter, Gold Marker, Carbon Marker

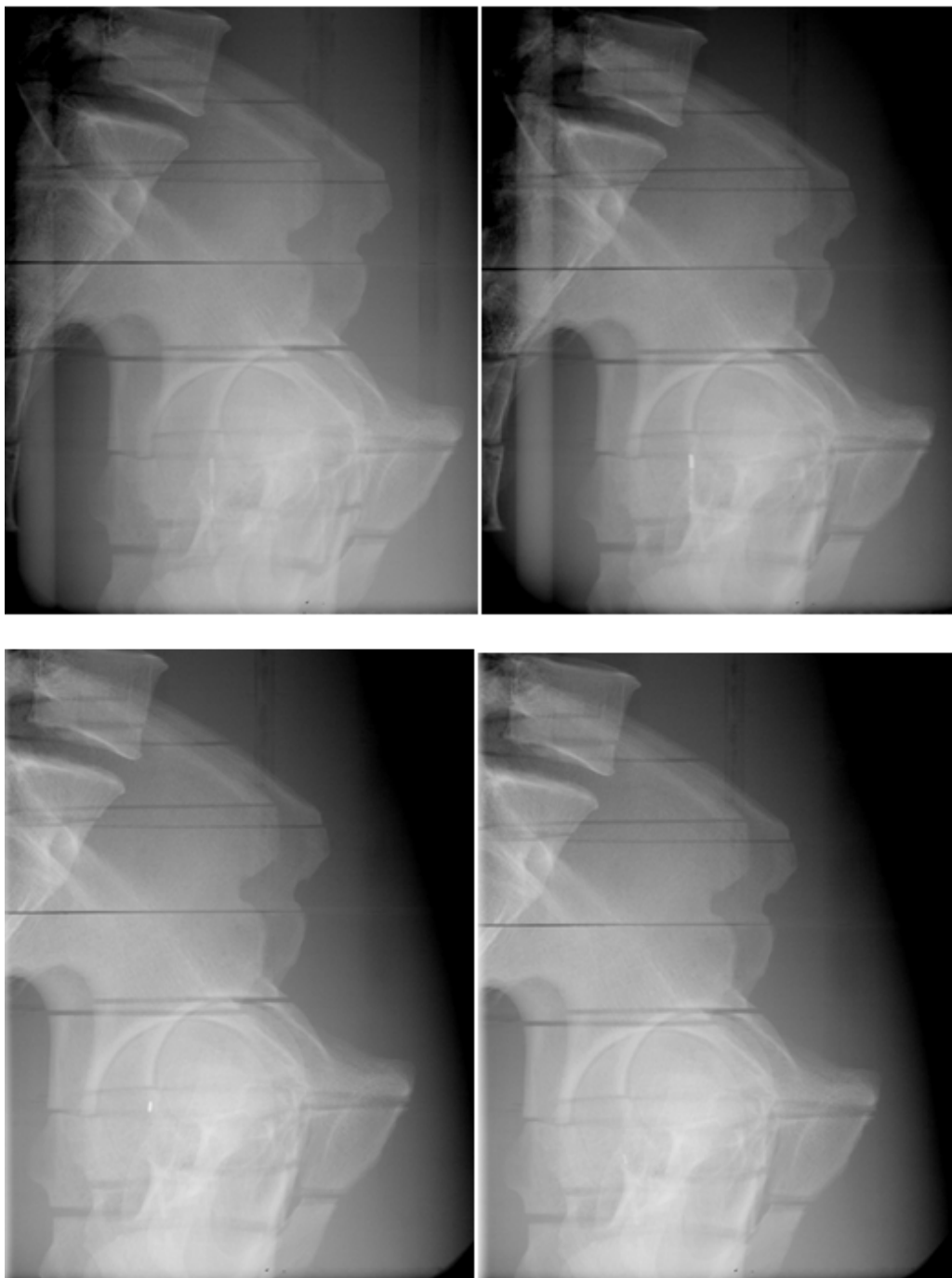


Figure 29 - kV Lateral images. From top to bottom: Commercially Available Dosimeter, Modified Dosimeter, Gold Marker, Carbon Marker

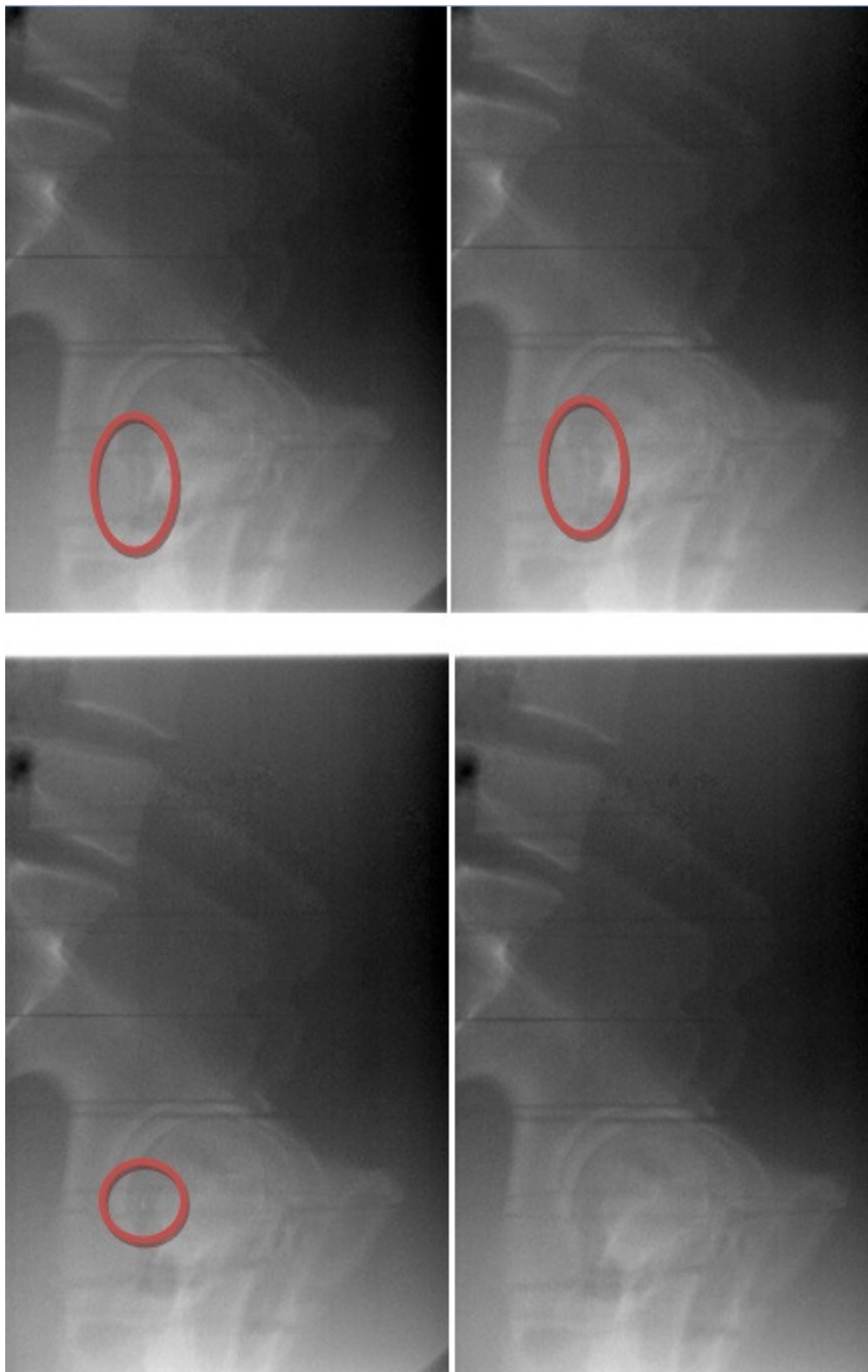


Figure 30 - MV Lateral images. From top left to bottom right: Commercially Available Dosimeter, Modified Dosimeter, Gold Marker, Carbon Marker

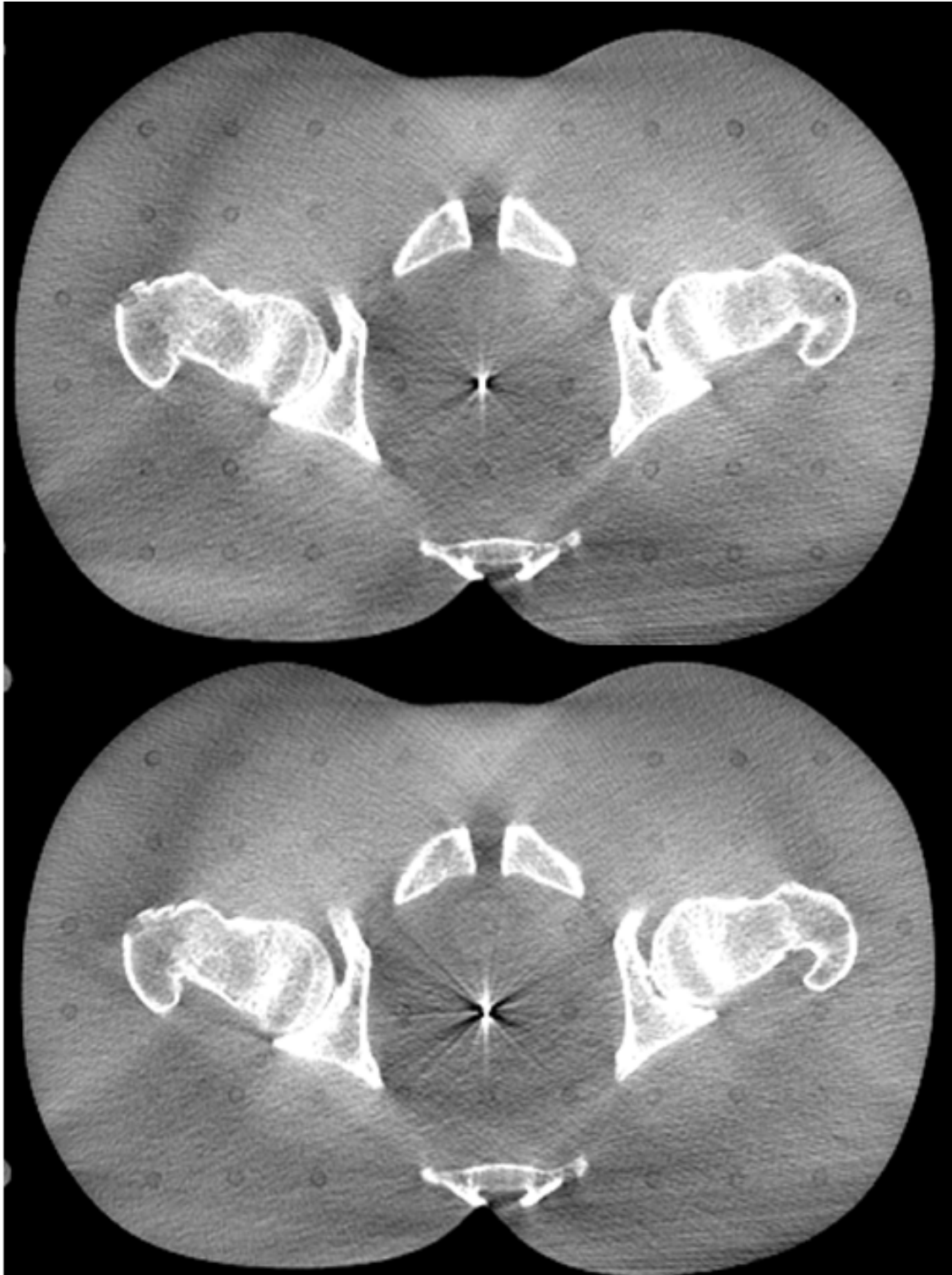


Figure 31 - CBCT Slice of Commercial Dosimeter (top), Modified Dosimeter (bottom)

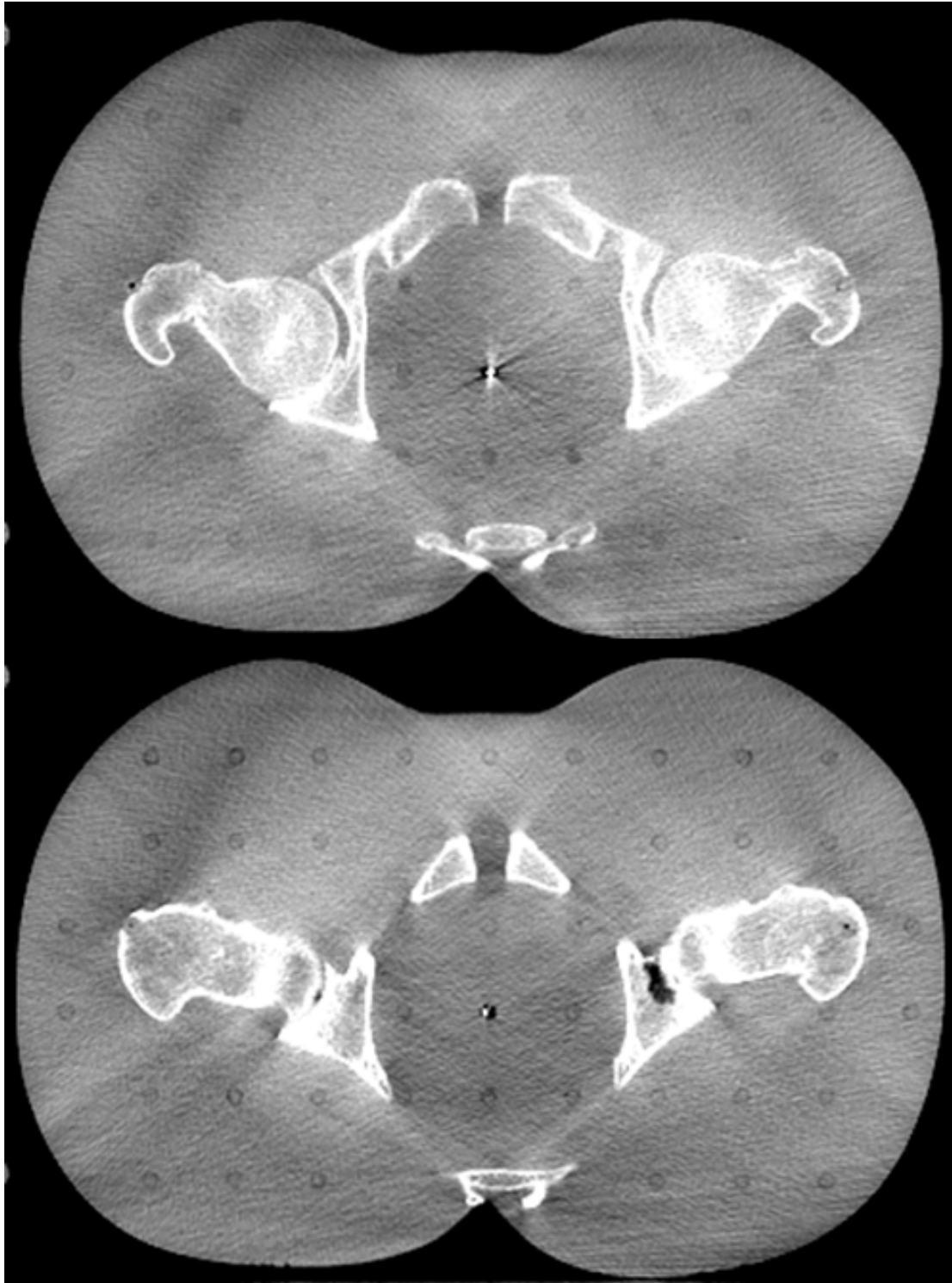


Figure 32 - CBCT Slice of Gold Marker (top), Carbon Marker (bottom)

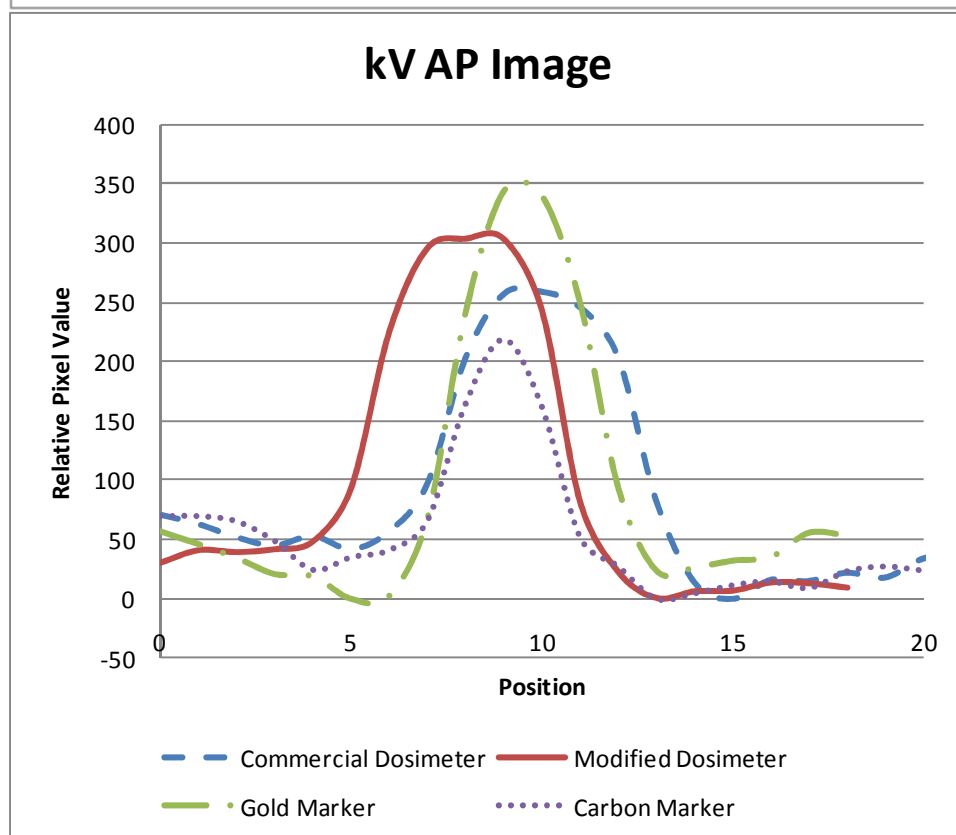
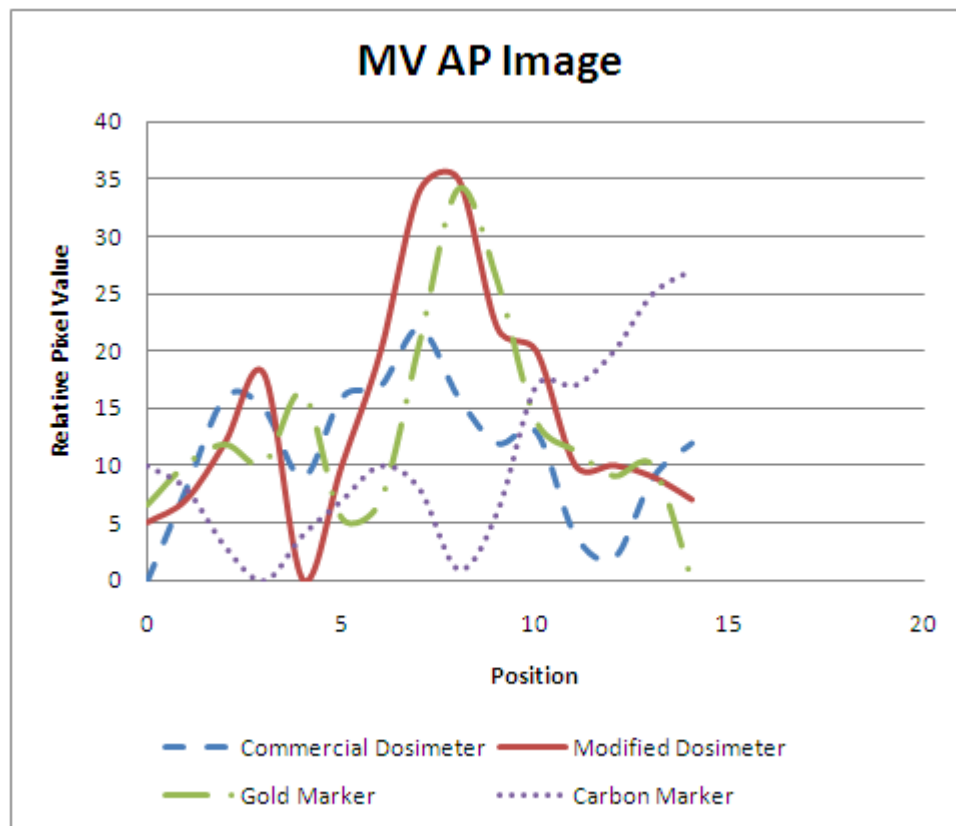


Figure 33 - Line profiles of the AP images. The gold marker and modified dosimeter show comparable results.

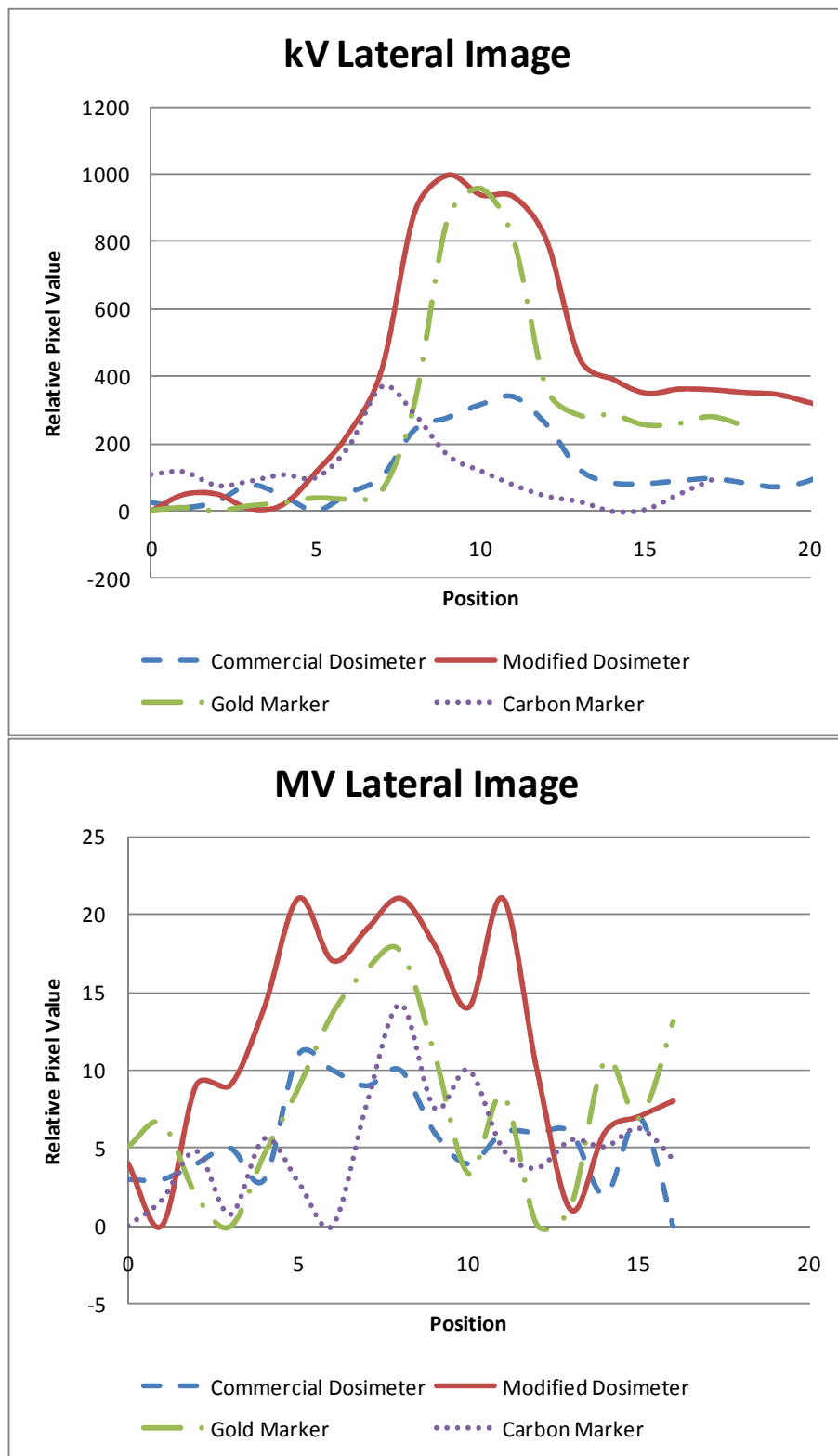


Figure 34 - Line profiles of the lateral images. The gold marker and modified dosimeter show comparable results.

All markers show good visibility in kV AP images (Figure 26). On the kV lateral images (Figure 29), the carbon marker cannot be seen. On the MV AP images (Figure 27), the gold marker and modified dosimeter can be clearly seen, though the modified dosimeter is easier to find due to it being much larger than the gold marker. A shadow of the commercial dosimeter is barely visible and the carbon marker is not visible. On the MV lateral images (Figure 30), the markers are harder to find, but only the carbon marker is completely impossible to see. The gold marker and modified dosimeter are considerably easier to see than the commercial dosimeter, of which only a shadow is visible. On the CBCT images (Figure 31 and Figure 32), the modified dosimeter shows the largest star artifact with the carbon marker showing almost none.

The line profiles (Figure 33 and Figure 34) show that the modified dosimeter and gold marker behave comparably for all imaging types. The relative pixel difference of the modified dosimeter and gold marker are similar, but the modified dosimeter has a larger area of difference, further increasing its visibility. Though the carbon marker and commercial dosimeter underperform the gold marker and modified dosimeter on the imaging tests, the line profiles on the kV images show pixel differences that would still clearly be visible.

Based upon these results, the modified dosimeter can be used as a fiducial marker for both kV and MV imaging applications. In the MV images, the gold fiducial marker has a greater contrast difference from background than the modified dosimeter; however, the modified dosimeter's larger size makes it more easily viewable. The CT artifacts are concerning, however the commercially available dosimeter also shows such

artifacts, so the increase in them via modification should not significantly affect their use.

Read Range Study

It was found that the read range of both the commercial and modified dosimeters was 9 cm. At 10 cm, the dosimeters were detected, but could not be read. Beyond 10 cm, the dosimeters were not even detected by the wand apparatus. This result demonstrates that the modification did not affect the depth at which the dosimeters could be read. It was a little concerning, however, in that the manufacturer had stated that the dosimeters had a 15 cm read range. The manufacturer was contacted about this discrepancy and it was discovered that their read range tests used a new model of wireless wand. This new model produces an electromagnetic wave with higher amplitude, and is more sensitive in its read response. The manufacturer stated that the new model wand extended the range of the dosimeters by roughly 4 cm, bringing the results of this work closer to the manufacturer's stated values.

Energy Dependence Study

The results of the energy dependence study are shown in Table 2. There is a small variation between the energy response at 6MV and 15MV. Beyer *et al.* (2008) found that 15MV responded 0.5% higher than 6MV for the commercial dosimeter, consistent with the results of this study.

Table 2 - Energy Dependence Study				
Energy	n	Commercial Dosimeter	Modified Dosimeter	p-value
6MV	9	0.00%	0.00%	
15MV	9	0.67%	-1.43%	0.0136

Table 2 - Results of the Energy Dependence Study for both the commercial and modified dosimeter

The modified dosimeter responds differently to 15MV than the commercial dosimeter, under responding by -1.43% instead of over-responding by 0.67%. This difference is statistically significant ($p=0.0136$), but it is not believed to result from any modification of the dosimeter. Each batch of MOSFETs has specific energy dependence characteristics. Sometimes the dosimeters over respond to higher energies, sometimes they under respond. According to the manufacturer, typical values are $\pm 1\%$. The MOSFETs used to create the modified dosimeter probably had different intrinsic energy dependence than the MOSFETs used to create the commercial dosimeters. However, even if the difference is caused by the dosimeter modification, the resulting energy dependence is still not clinically significant. The dosimeters are guaranteed by the manufacturer to be within $\pm 5\%$. The dosimeters are calibrated to split the difference between high and low energy photons, so if used for 6MV photons, the modified dosimeters would read $1.43\%/2 = 0.72\%$ and if used for 15MV photons, they would read -0.72% . This error, combined with the 2% inherent uncertainty in readings, still places the dosimeter's characteristics well within the $\pm 5\%$ specified range.

Rotational Angular Dependence Study

The rotational angular dependence of the dosimeter is reported in Table 3 and graphically in Figure 35.

Table 3 - Rotational Angular Dependence				
Rotational Angle	n	Commercial Dosimeter	Modified Dosimeter	p-value
0	3	0.00%	0.00%	
40	3	-0.22%	-0.48%	0.843
80	3	-2.98%	-4.57%	0.302
90	3	-3.93%	-4.91%	0.485
120	3	-2.01%	-1.85%	0.902
160	3	-0.07%	0.41%	0.718
180	3	1.75%	1.37%	0.773
200	3	1.61%	-0.63%	0.192
240	3	-1.34%	-0.93%	0.756
270	3	0.37%	-1.00%	0.357
280	3	-0.25%	-1.79%	0.314
320	3	2.32%	-0.19%	0.162

Table 3 - Rotational Angular Dependence of both the Commercial and Modified Dosimeters

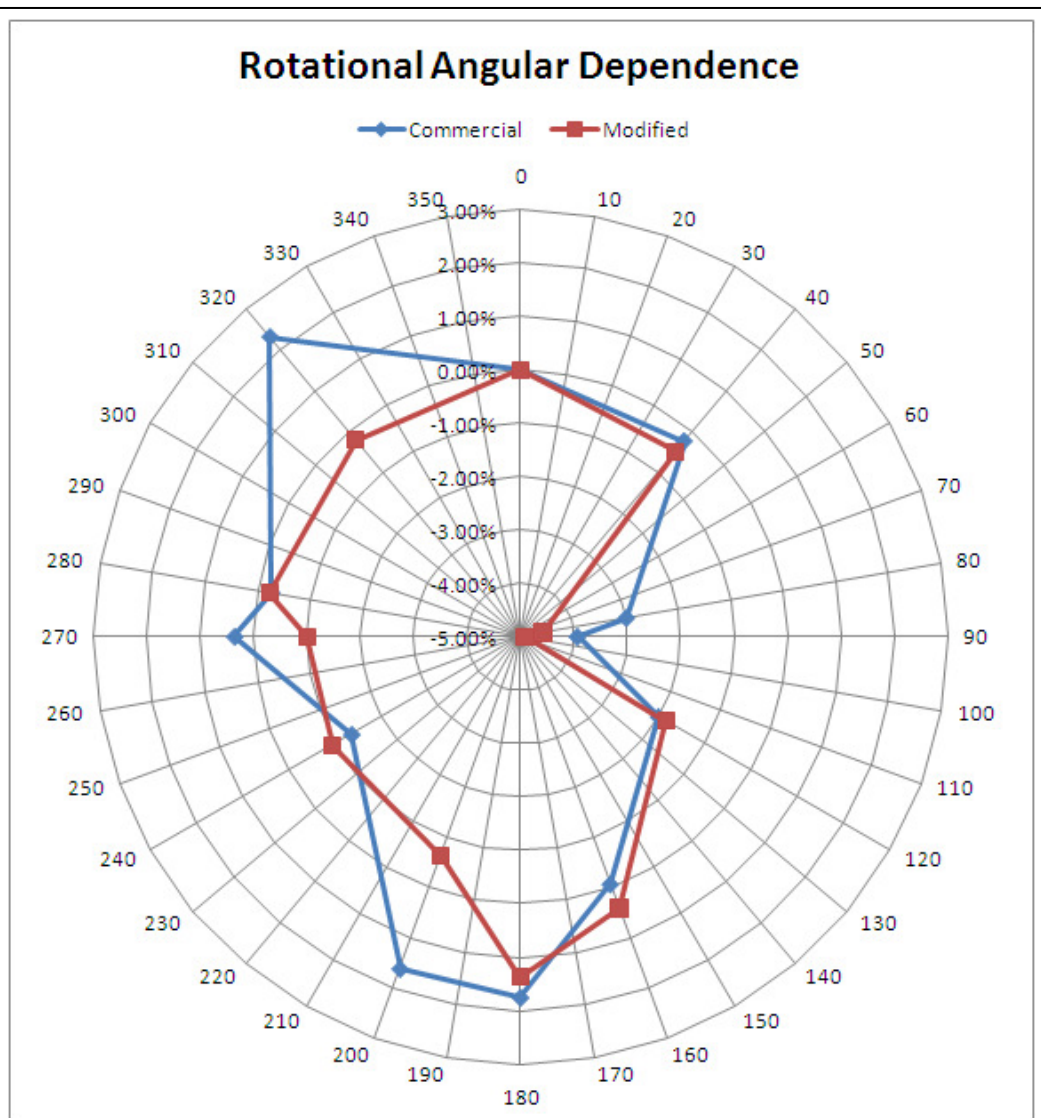


Figure 35 - Rotational Angular Dependence

The dosimeters are largely in agreement with each other, with the greatest variation occurring at 200° and 320°, which show a difference of 2.24% and 2.51%, respectively. These differences are not statistically significant ($p=0.192$ and $p=0.162$, respectively). In terms of the actual readings by the dosimeters, rotational angular response is generally within $\pm 2\%$, with the exception of 90°, which reads -3.93% for the commercial and -4.91% for the modified. The dosimeters are known to under-respond

in this direction, though this study found higher variation than had been previously reported (-2.5% (Beyer 2008) and -1.2% (Briere 2007)). This result is a little concerning since a systematic -4.91% error could cause readings to exceed the manufacturer's specified $\pm 5\%$ guarantee. However, as with the energy dependence, the dosimeters are calibrated to split the difference between the 0° and 90° reading, so that a 90° beam would actually read as $-4.91\%/2 = -2.45\%$. Also, typical radiation therapy treatments are given with a wide range of beams from multiple angles. Since 90° is the only angle that under responds so much, beams incident at other angles would serve to average out the under response from 90° . Though the dosimeter's intrinsic characteristics are interesting, the focus of this study is in determining how the modification of the dosimeter affected its dosimetry characteristics. This test showed that the modification of the dosimeter did not alter its rotational angular dosimeter characteristics.

It is unexpected that the 90° and 270° rotations are not in greater agreement. It is possible that the MOSFETs are soldered on to the circuitry at this angle, which is why the attenuation is seen here and at no other angle.

Longitudinal Angular Dependence Study

The longitudinal angular dependence of both the commercial and modified dosimeters is shown in Table 4.

Table 4 - Longitudinal Angular Dependence				
Longitudinal Angle	n	Commercial Dosimeter	Modified Dosimeter	p-value
290	3	-4.85%	-5.15%	0.819
310	3	-1.97%	-2.63%	0.625
330	3	-1.73%	-0.15%	0.305
350	3	-1.81%	1.55%	0.101
0	3	0.00%	0.00%	
10	3	0.24%	0.74%	0.707
30	3	-1.96%	-1.31%	0.630
50	3	-3.54%	-1.72%	0.256
70	3	-5.31%	-5.23%	0.951

Table 4 - Longitudinal Angular Dependence of both the Commercial and Modified Dosimeter

The longitudinal angular responses are largely in agreement, with the greatest discrepancy occurring at 350°. At 350°, the commercial dosimeter under-responds by -1.81% compared to 0° and the modified dosimeter over-responds by 1.55%. The difference is not statistically significant ($p=0.101$) and it seems unlikely that modifying the dosimeter would affect only the 350° angle and no others. With the exception of 30°, the dosimeter's response to these angles has never been reported, but Beyer *et al.* (2008) found the response at 30°, 90° and 270° to be -0.6%, -3.6% and -6.0%, respectively. These values seem to be in agreement with this data, though 70° is already higher than the 90° measurement found by Beyer *et al.* (2008). Again, however, the focus of this work is in the comparison of the commercial and modified dosimeter. Based upon these

results, the modification of the dosimeter did not alter its longitudinal angular dependence.

Azimuthal Angular Dependence

The angular dependence in the azimuthal direction for both the commercial and modified dosimeters is shown in Table 5.

Table 5 - Azimuthal Angular Dependence Relative to Rotational 0				
Azimuthal Angle	n	Commercial Dosimeter	Modified Dosimeter	p-value
290	3	-5.04%	-4.63%	0.756
310	3	-5.88%	-4.83%	0.459
330	3	-2.64%	-4.43%	0.261
350	3	-4.81%	-4.00%	0.556
0	3	-5.28%	-4.21%	0.452
10	3	-5.33%	-4.99%	0.796
30	3	-5.49%	-4.51%	0.485
50	3	-5.41%	-4.68%	0.592
70	3	-7.73%	-6.43%	0.377

Table 5 - Azimuthal Angular Dependence of both the Commercial and Modified Dosimeters. The data is reported relative to a 0° rotation, 0° longitudinal angle

As mentioned in the Methods and Materials section, all data is relative to a 0° rotation, 0° longitudinal angle. Since azimuthal angles are longitudinal angles at a 90° rotation, the azimuthal angle of 0° should roughly correspond to what was found for the 90° angle in the rotational angular dependence study. Upon analyzing this data, it seems that there is a systematic difference between the commercial and modified dosimeter with the commercial dosimeter reading roughly -5% and the modified dosimeter reading roughly -4%. Therefore, the data are also presented as a difference from the azimuthal 0° angle in Table 6.

Table 6 - Azimuthal Angular Dependence Relative to Azimuthal 0				
Azimuthal Angle	n	Commercial Dosimeter	Modified Dosimeter	p-value
290	3	0.25%	-0.42%	0.620
310	3	-0.59%	-0.61%	0.988
330	3	2.64%	-0.22%	0.132
350	3	0.48%	0.21%	0.837
0	3	0.00%	0.00%	
10	3	-0.05%	-0.78%	0.592
30	3	-0.21%	-0.30%	0.945
50	3	-0.12%	-0.47%	0.790
70	3	-2.44%	-2.21%	0.861

Table 6 - Azimuthal Angular Dependence for both the Commercial and Modified Dosimeter. Data presented is the difference between the angular readings and the Azimuthal 0° angular reading.

The azimuthal angular dependences of both the commercial and modified dosimeter are largely in agreement with the exception of the reading at 330° for which the commercial dosimeter read 2.64% (relative to the commercial dosimeter's azimuthal 0° reading) and the modified dosimeter read -0.22% (relative to the modified dosimeters' azimuthal 0° reading). This result is not statistically significant ($p=0.132$). The values relative to the azimuthal 0° are all within $\pm 1\%$, except for 70°, which reads as roughly -2% for both the commercial and modified dosimeters. It is interesting that the azimuthal angular dependence is not similar to the longitudinal angular dependence, and is more a function of the rotational angular dependence than any other factor. These results again show that the modification of the dosimeter did not alter the azimuthal angular dependence.

CONCLUSIONS

Suitability of Modified Dosimeter as a Fiducial Marker

Based upon the imaging portion of this study, the modified dosimeter is visible on kV, MV and CBCT images. Visibility is comparable to the gold marker in the MV images. The modified dosimeter does have a disadvantage in terms of the artifacts produced in the CBCT images. The artifacts produced by the modified dosimeter were larger than those produced by the commercially available dosimeter and by the gold marker. These artifacts could be particularly problematic during initial CT simulation of the patient for treatment planning purposes. Artifacts during CT simulation are an issue for all fiducial markers, however, and are certainly not limited to just the modified dosimeter. It will be up to the physician to determine whether the detriments of additional artifacts from the modified dosimeter are worth the advantages of an *in vivo* dosimeter capable of being used for IGRT.

Effect of Modification on Dosimeter Properties

The modified dosimeter showed no significantly different characteristics than the commercially available dosimeter. The angles in the rotational, longitudinal and azimuthal direction were in surprisingly close agreement. The difference between the energy dependence of the dosimeters was statistically significant, however the energy dependence of the dosimeters is dependent upon the manufacturing lot from which the MOSFETs came. It seems more likely that the difference is explained by the fact that the modified dosimeters' MOSFETs came from a different manufacturing lot than the commercial dosimeters than that the modification of the dosimeter had an effect on the energy dependence. To test this assumption, dosimeters from the same MOSFET

manufacturing lot could be chosen and half modified, half left unmodified. Ultimately, however, this test is irrelevant. An energy dependence of -1.43%, as was found for the modified dosimeter will not have any effect on its usability as a dosimeter since energy dependences of $\pm 1\%$ are frequently found in the commercially available dosimeter. Therefore, even if the modification of the dosimeter were causing the energy dependence, its usability as a dosimeter would not be in jeopardy.

Future Work

Future work could focus on altering the materials used in creating the fiducial marker to further improve its visibility. Though it seems that the wire wrapped design is a good design to avoid hindering the wireless read range, a material other than gold could possibly be used. The material would need to be sufficiently ductile to be shaped around the antenna. Also, since Compton interactions dominate at MV level x-rays, the material need not be high-Z, but must have a high physical density. A high density alloy might offer an even greater visibility at lesser cost than the gold.

Recommendations

It is the opinion of this author that there is little reason not to incorporate this modification into the existing product. Based upon this work, it seems likely that the modified dosimeter will provide all the advantages of an *in vivo* dosimeter that the original commercial dosimeter provided, while providing the benefit of an MV-visible fiducial marker for IGRT.

BIBLIOGRAPHY

- Almond, Peter, Peter Biggs, B.M. Coursey, W.F. Hanson, M. Saiful Huq, Ravinder Nath, D.W.O. Rogers. AAPM's TG-51 Protocol for Clinical Reference Dosimetry of High-Energy Photon and Electron Beams. *Medical Physics*. Volume 26, September 1999, Pages 1847-1870.
- Beddar, A S, M Salehpour, T M Briere, H Hamidian, M T Gillin. Preliminary Evaluation of Implantable MOSFET Radiation Dosimeters. *Physics in Medicine and Biology*. Volume 50, January 2005, Pages 141-149.
- Beyer, Gloria P., Charles W. Scarantino, Bradley R. Prestidge, Amir G. Sadeghi, Mitchell S. Anscher, Moyed Miften, Tammy B. Carrea, Marianne Sims, Robert D. Black. Technical Evaluation of Radiation Dose Delivered in Prostate Cancer Patients as Measured by an Implantable MOSFET Dosimeter. *International Journal of Radiation Oncology Biology Physics*, Volume 69, Issue 3, 1 November 2007, Pages 925-935.
- Beyer, Gloria P., Greg G. Mann, Jay A. Pursley, Eric T. Espenhahn, Caroline Fraisse, Devon James Godfrey, Mark Oldham, Tammy B. Carrea, Natasha Bolick, Charles W. Scarantino. An Implantable MOSFET Dosimeter for the Measurement of Radiation Dose in Tissue During Cancer Therapy. *IEEE Sensors*, Volume 8, Issue 1, 1 January 2008, Pages 38-51.
- Black, Robert D., Charles w. Scarantino, Gregory G. Mann, Mitchell S. Anscher, Robert D. Ornitz, Benjamin E. Nelms. An Analysis of an Implantable Dosimeter System for External Beam Therapy. *International Journal Radiation Oncology Biology Physics*. Volume 63, Issue 1, 2005, Pages 290-300.

- Bortfeld T, H Paganetti. The biologic relevance of daily dose variations in adaptive treatment planning. *International Journal of Radiation Oncology Biology Physics*, Volume 65, Issue 3, July 2006, Pages 899-906.
- Brahme A. Dosimetric precision requirements in radiation therapy. *Acta Radiologica Oncology*, Volume 23, Issue 5, 1984, Pages 379-391.
- Briere, Tina Marie, A. Sam Beddar, Michael T. Gillin, Evaluation of Precalibrated Implantable MOSFET Radiation Dosimeters for Megavoltage Photon Beams. *Medical Physics*, Volume 32, Issue 11, November 2005, Pages 3346-3349.
- Briere, Tina Marie, Michael T. Gillin, A. Sam Beddar. Implantable MOSFET Detectors: Evaluation of a New Design. *Medical Physics*, Volume 34, Issue 12, December 2007, Pages 4585-4590
- Fagerstrom, Jessica M., John A. Micka, Larry A. DeWerd. Response of an Implantable MOSFET Dosimeter to Ir192 HDR Radiation. *Medical Physics*. Volume 35, Issue 12, December 2008, Pages 5729-5737.
- Kry, Stephen F., Michael Price, Zhonglu Wang, Firas Mourtada, Mohammad Salehpour. Investigation into the use of a MOSFET Dosimeter as an Implantable Fiducial Marker. *Journal of Applied Clinical Medical Physics*, Volume 10, Issue 1, Winter 2009, Pages 22-32
- Scalchi, Paolo, Roberto Righetto, Carlo Cavedon, Paolo Francescon. Direct tumor *in vivo* dosimetry in highly-conformal radiotherapy: A feasibility study of implantable MOSFETs for hypofractionated extracranial treatments using the Cyberknife® system. *Medical Physics*, Volume 37, Issue 4, April 2010, Pages 1413-1423.
- Scarantino, Charles W., David M. Ruslander, Christopher J. Rini, Gregory G. Mann, H. Troy Nagle. Robert D. Black. An Implantable Radiation Dosimeter for use in

External Beam Radiation Therapy. *Medical Physics*, Volume 31, Issue 9,
September 2004, Pages 2658-2671.

Scarantino, Charles W., Christopher J. Rini, Migdalia Aquino, Tammy B. Carrea, Robert D. Ornitz, Mitchell S. Anscher, Robert D. Black. Initial Clinical Results of an In Vivo Dosimeter During External Beam Radiation Therapy. *International Journal Radiation Oncology Biology Physics*, Volume 62, Issue 2, 2005, Pages 606-613.

Scarantino, Charles W., Bradley R. Prestidge, Mitchel S. Anscher, Carolyn R. Ferree, William T. Kearns, Robert D. Black, Natasha G. Bolick, Gloria P. Beyer. The Observed Variance Between Predicted and Measured Radiation Dose in Breast and Prostate Patients Utilizing an In Vivo Dosimeter. *International Journal of Radiation Oncology Biology Physics*, Volume 72, Issue 2, 1 October 2008, Pages 597-604.

VITA

Joseph Stevenson Dick was born on July 11, 1985, the son of Brian Stevenson Dick and Dawn Camille Dick. He graduated as valedictorian of the International Baccalaureate School in Bartow, FL and was designated a National Merit Scholar. He attended the University of Florida on a National Merit Scholarship and received a Bachelor of Science in Physics and a Bachelor of Science in Business Administration in May, 2008. In August of 2008 he entered The University of Texas Health Science Center at Houston Graduate School of Biomedical Sciences.

Permanent address:

5725 Lake Breeze Ave.

Lakeland, FL 33809